ICARUS 76, 295–334 (1988)

Dynamics of the Uranian and Saturnian Satellite Systems: A Chaotic Route to Melting Miranda?[1]

STANLEY F. DERMOTT

Center for Radiophysics and Space Research, Space Sciences Building, Cornell University, Ithaca, New York 14853

RENU MALHOTRA

Department of Physics, Clark Hall, Cornell University, Ithaca, New York 14853

AND

CARL D. MURRAY

Astronomy Unit, School of Mathematical Sciences, Queen Mary College, University of London, Mile End Road, London E1 4NS, United Kingdom

Received July 6, 1987; revised February 15, 1988

We argue that the anomalously large inclination of Miranda, the postaccretional resurfacing of both Miranda and Ariel, and the anomalously large eccentricities of the inner Uranian satellites indicate that resonant configurations once existed in the Uranian satellite system that have since been disrupted. Similar anomalies that cannot be accounted for by the present resonant configurations also exist in the Saturnian satellite system, and we suggest that temporary resonances existed in the past in that system as well. Using classical methods of analyzing the dynamics of resonance, we show how temporary capture into a second- or higher-order resonance can produce large increases in e and I on comparatively short time scales. However, these methods may not provide a complete description of resonances in the Uranian satellite system. Since values of $J_2(R_p/a)^2$ for the inner Uranian satellites are small while their mass ratios, m/M, are large, resonances in the Uranian system are not always well separated. For resonances that are not well separated, it is not possible to analyze the dynamics using a disturbing function that is truncated to the extent that it contains only a single resonant argument. We have made some progress with this problem using the Cornell National Supercomputer to simulate the dynamics numerically. We find that capture into resonance may result in chaotic motion. We discuss two mechanisms that can be invoked to disrupt high-order resonances: the "spontaneous" disruption of chaotic resonances and the disruption of resonances due to the tidal damping of a satellite's eccentricity while the satellite is in a nonsynchronous spin state. © 1988 Academic Press, Inc.

I. INTRODUCTION

Since the exploration of the outer solar system by the Voyager spacecraft, our understanding of solar system dynamics has been changed in important ways by the following observations and findings. First, as predicted by Peale *et al.* (1979), the Jovian satellite Io was revealed by the Voyager cameras to be actively volcanic (Smith *et al.* 1979), while some small, icy satellites, particularly the Saturnian satellite Enceladus (Smith *et al.* 1981) and the Uranian sat-

[1] Presented at a conference celebrating the 300th anniversary of the publication of Newton's *Principia*, held at the Royal Greenwich Observatory in July 1987.

0019-1035/88 $3.00

ellites Miranda and Ariel (Smith *et al.* 1986), show evidence of widespread melting. Second, Wisdom (1982, 1983), Dermott and Murray (1983), and Milani and Nobili (1985) have drawn attention to the role of chaos in the evolution of asteroidal orbits. We show in this paper that in tracing the orbital and thermal evolution of the Uranian satellites, we need to consider both eccentricity damping and the role of chaos.

While tidal heating due to the damping of its orbital eccentricity successfully accounts for Io's volcanism, this mechanism cannot be usefully applied to the present orbital configurations of either Miranda or Ariel. An important consequence of the work on the tidal heating of Io by Yoder (1979) and Yoder and Peale (1981) is the demonstration that the thermal output of the satellite is ultimately determined by the rate of tidal dissipation in the planet. Thus, Io's volcanism provides observational evidence that significant tidal dissipation occurs in the interior of at least one of the giant planets, providing a mechanism for the formation of the orbit–orbit resonances in that system. Unlike the Jovian and the Saturnian satellite systems, the satellite system of Uranus is devoid of stable orbit–orbit resonances. The simplest explanation for this allows that the Q of Uranus is too high to produce significant orbital evolution. However, we argue (a) that several features indicate that resonant configurations once existed in the Uranian satellite system and (b) that since these configurations no longer exist they must have been disrupted. These features are (1) the anomalously large inclination of Miranda, (2) the postaccretional resurfacing of both Miranda and Ariel, and (3) the anomalously large eccentricities of the inner satellites, Miranda, Ariel, and Umbriel (Dermott 1984, Squyres *et al.* 1985). Similar anomalies are found in the Saturnian system. These include (1) the large eccentricity of Mimas, (2) the large initial inclinations of Mimas and Tethys, where by "initial" we mean the inclinations that the satellites had before encountering the inclination-type resonance in which they are now trapped (Allan 1969), and (3) the postaccretional resurfacing of Enceladus. These anomalies cannot be accounted for by the existing resonances and this leads us to suggest that other resonances also existed in the Saturnian system before the present resonances were established.

In Section II, we investigate the changes in the satellite orbital radii that could have been produced by tidal dissipation in the planets. There are many reasons why the orbital histories are uncertain: (1) lack of knowledge of the magnitude of the tidal dissipation function, Q_p, and of its variability with time, (2) lack of knowledge of the amplitude and frequency dependence of Q_p, (3) imprecise knowledge of the satellite masses, particularly those of Miranda, Ariel, and Enceladus. These and other uncertainties make it difficult to determine the exact sequence in which the various orbit–orbit resonances may have been encountered. We confine our discussion to what we consider to be the main features of the possible evolutionary schemes.

In Section III we discuss the approaches that have been used to study the dynamics of orbital resonance. Previous discussions of the orbital evolution of the Uranian satellite system have been oversimple from two viewpoints. (1) Since the values of $J_2(R_p/a)^2$ of the inner Uranian satellites are small while their mass ratios, m/M, are large, resonances in the Uranian system are not always well separated (Dermott and Murray 1983, Dermott 1984a,b). Thus, it is not always possible to analyze the dynamics of resonance in the Uranian system using a disturbing function that is truncated to the extent that it contains only a single resonant argument. By using the Cornell National Supercomputer to simulate the dynamics numerically, we show that capture into resonance in the Uranian system may result in chaotic motion. (2) In Section IV we show that the number of possibly significant resonances that needs to be considered has been underestimated. Second-order, third-order and, possibly, even higher order resonances may have been strong enough to withstand the forces generated by tidal dissipation in the planet.

In Section V we demonstrate that, provided a particular resonance is strong enough to withstand the drag forces acting on the satellites, the increases in the eccentricities and inclinations that occur on capture into resonance, and the time scales on which these increases occur, are determined largely by the tidal torques exerted on the satellites and are not strongly dependent on the order of the resonance. In fact, counter to intuition, high-order resonances are actually more effective than low-order resonances at increasing the eccentricities and inclinations. Large increases in e and I can be produced by high-order resonances on comparatively short time scales.

In Section VI we discuss how Miranda's eccentricity could have been increased by the temporary trapping of the satellite in a second-order (or higher-order) resonance with an outer satellite. We also point out that, paradoxically, small, cold, icy satellites are more likely to be melted by eccentricity damping than some of their larger neighbors. The major dynamical problem presented to us by the Uranian satellite system is the anomalously large inclination of Miranda. We discuss how a temporary resonance could have produced this large inclination.

A detailed understanding of the orbital and thermal evolution of Miranda requires an appreciation of the time scales of a number of significant, sometimes competing, processes. These are discussed in Section VII. The processes include (1) the heating and cooling time scales of the satellites, (2) changes in the semimajor axes due to tidal dissipation in both the planet and the satellites, (3) increases in the orbital elements due to resonant interactions between satellites, and (4) damping of the eccentricities due to tidal dissipation in the satellites. Some of the time scales are dependent on the spin states of the satellites.

Finally, we recognize that temporary resonant trapping cannot be invoked unless mechanisms exist that act to disrupt resonances. Satellite systems are dynamically 10^2 to 10^3 times older than the planetary system (the dynamical age of a system is determined by the number of orbits around the central body that the secondaries in the system have completed) and we consider that the stability of resonant configurations over periods as long as 10^{10} to 10^{12} orbits, particularly those configurations for which the motion is chaotic, needs to be proved rather than assumed. We have observed that in the case of a chaotic resonance, disruption can be spontaneous. In Section VIII we discuss whether tidal dissipation in the satellite while the satellite is in a nonsynchronous spin state may be important enough to disrupt high-order resonances.

II. TIDAL EVOLUTION

The rate of change of the semimajor axis of a satellite with time due to tidal dissipation in a planet is given by

$$\left(\frac{da}{dt}\right)_t = \operatorname{sign}(N - n)3k_{2p}\left(\frac{G}{M}\right)^{1/2}\frac{R_p^5}{Q_p}\frac{m}{a^{11/2}}, \tag{1}$$

where G is the gravitational constant; N, M, R, Q_p, and k_{2p} are, respectively, the spin frequency, mass, radius, tidal dissipation function, and Love number of the planet; and m, n, and a are the mass, mean motion, and semimajor axis of the satellite (Munk and MacDonald 1960). We can relate the Love number, k_{2p}, to the dynamical oblateness, J_2, through

$$k_{2p} = 4\pi G\rho_p J_2 N^{-2}, \tag{2}$$

where ρ_p is the density of the planet. On integrating Eq. (1), assuming that the tidal dissipation function is amplitude and frequency independent, we obtain

$$a_0^{13/2} - a_i^{13/2} = \operatorname{sign}(N - n)C_p m t \tag{3}$$

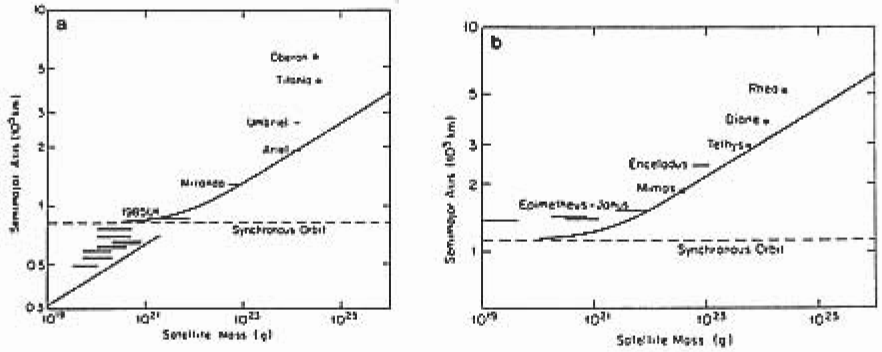

FIG. 1. Distribution of masses in the inner regions of the satellite systems of (a) Uranus and (b) Saturn. If tidal evolution has been appreciable, then the solid curves place bounds on the satellite distributions. The linear portions of these curves have slopes of 2/13. The masses of the small satellites were estimated from their radii using densities of 1.6 g cm^{-3} for the Uranian satellites and 1.1 g cm^{-3} for the Saturnian satellites. We assume that these masses are uncertain by a factor of 2.

when the satellite evolves from an initial orbital radius a_i to a final orbital radius a_o in a time t, and C_p is a positive constant peculiar to the planet.

If tidal forces have had a significant role in the orbital evolution of a particular satellite system, then Eq. (3) places a bound on the distribution of the satellites in that system. On a logarithmic plot of semimajor axis against mass, with $a_i = a_{sync}$, where a_{sync} is the radius of the synchronous orbit, Eq. (3) defines a near-linear curve of slope 2/13 that passes through that satellite for which $m/a^{13/2}$ is a maximum—see Fig. 1. If the orbit of this satellite is tidally evolved, then we expect the line, and its linear extrapolation to points below synchronous height, to divide the plot into two regions (Dermott 1971). Satellites above synchronous height can exist above or close to the line, but never below it. For satellites below synchronous height, the line defines the initial orbital radius of a satellite whose orbit would decay into the planet in a time t. Thus, satellites with initial orbital radii below the synchronous orbit and below the line would have been lost from the system, although it has been suggested that the orbital decay of those satellites led to the formation of the Uranian rings (Dermott *et al.* 1979).

The distributions of the satellites in the Uranian and Saturnian systems are shown in Fig. 1. Not only are these distributions consistent with those expected for tidally evolved satellite systems; in addition, the closeness of the inner satellites to the tidal demarcation lines suggests that significant orbital evolution due to tidal dissipation has actually occurred in both systems. The only anomaly is the position of 1985U1 in the Uranian system. This satellite clearly lies below the line that passes through Ariel. However, we have assumed that the tidal dissipation function Q_p is independent of the tidal frequency, $2(N - n)$. For most satellites, $N \gg n$ and any variation of Q_p with frequency can be neglected. The only exceptions are those satellites close to the synchronous orbit for which $N \approx n$. Thus, although the position of 1985U1 is anomalous, since it is very close to synchronous orbit we cannot use its position to place useful bounds on the orbital evolution of the other satellites.

If we assume that $t = 4.5 \times 10^9$ years, then from the present orbit of Ariel we deduce that

$$Q(\text{Uranus}) > 1.8 \times 10^4, \qquad (4)$$

while a similar calculation for Mimas yields

$$Q(\text{Saturn}) > 1.6 \times 10^4. \qquad (5)$$

The chief sources of tidal dissipation in the major planets are unknown. However, if the planets have solid cores, and this is certainly possible in the case of Uranus, then tidal dissipation in these cores may have been sufficient to account for the postulated orbital evolution (Dermott 1979a). If tidal dissipation was confined to a solid core of radius R_c, with tidal dissipation function Q_c and Love number k_{2c}, then the value of Q_c needed to produce the required energy dissipation is given by

$$Q_c = \left(\frac{R_c}{R_p}\right)^5 \frac{k_{2c}}{k_{2p}} F_p^2 Q_p, \qquad (6)$$

where F_p is a factor that allows for the enhancement of the tide in the core by the tide in the overlying ocean and for the effects of the density contrast between the core and the ocean (Dermott 1979a). For the model of the Uranian interior described by Hubbard (1984), we estimate that $R_c/R_p \sim 0.3$, $F_p^2 \sim 3$, and $k_{2c} \sim 0.25$. If we assume that orbital evolution has occurred at a constant rate over the age of the solar system, then the value of Q_c needed for significant orbital evolution is $\sim 10^2$.

For tidal dissipation in planetary cores, however, a constant rate of energy dissipation is unlikely. Uranus probably formed hot and the putative rocky core may have then been molten. Significant tidal dissipation in the core would have occurred only after the core cooled and solidified. Since the Q of near-solidus silicate rocks is between 1 and 10 (Murase and McBirney 1973, Sacks and Murase 1982), our requirements for significant orbital evolution are best stated as a demand that Q_c remained at the comparatively low value of ~ 10 for a period of one-tenth the age of the solar system rather than at the higher value of 10^2 for the whole age of the system.

If tidal dissipation has been appreciable, and Q_p is both amplitude and frequency independent, then the orbital radii of the Uranian and Saturnian satellites would have varied with time as shown in Fig. 2. In these plots, the time should be regarded as the integral

$$t' = \langle Q_p \rangle \int_0^t \frac{dt}{Q_p}, \qquad (7)$$

where $\langle Q_p \rangle$ is the value of the dissipation function averaged over the total time of orbital evolution, t. The origin of time in these

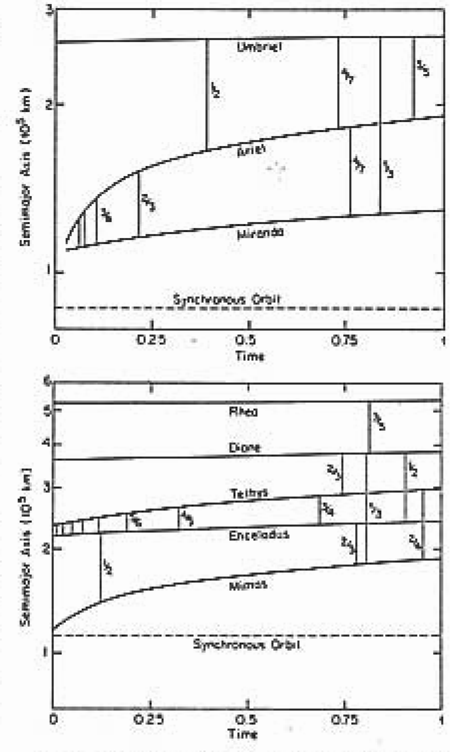

FIG. 2. Variations of orbital radii with time due to tidal dissipation in the planet for the satellites of Uranus and Saturn. All the first-order, and some of the second-order, and third-order resonances that the satellites could have encountered are marked with vertical lines. The Saturnian satellite pairs, Mimas–Tethys and Enceladus–Dione, are, at present, trapped in a second-order (2:4) II' resonance and a first-order (1:2) e resonance, respectively.

TABLE I

TIDAL TORQUES ON SATELLITES

Satellite	Semimajor axis, a ($\times 10^3$ km)	m/M ($\times 10^7$)	$m/a^{13/2}$ ($\times 10^{43}$ cgs)	Radius (km)	Free I (deg)	Free e	T_c/Q_s (10^6 years)
Miranda[a]	129.8	7.9 ± 2.1	1.27 ± 0.33	242	4.34	0.0013	2
Ariel	191.2	145 ± 21	1.87 ± 0.27	580	0.041	0.0012	1
Umbriel	266.0	153 ± 22	0.23 ± 0.03	595	0.13	0.0039	7
Titania	435.8	401 ± 15	0.024 ± 0.001	805	0.079	0.0011	50
Oberon	582.6	349 ± 12	0.0032 ± 0.0001	775	0.068	0.0014	400
Mimas[b]	185.5	0.659 ± 0.010	0.0675 ± 0.0011	198.5	1.53	0.0202	3
Enceladus	238.0	1.4 ± 0.5	0.028 ± 0.011	251	0.0045	0.0001	6
Tethys	294.7	10.95 ± 0.15	0.0554 ± 0.0007	524	1.09	0.0000	1
Dione	377.4	18.5 ± 0.5	0.0187 ± 0.0005	559	0.017	0.0022	5
Rhea	527.0	43.8 ± 2.6	0.0051 ± 0.0003	764	0.35	0.0003	10

[a] Masses of the Uranian satellites are from Anderson *et al.* (1988); eccentricities and inclinations are from Laskar and Jacobson (1988).

[b] Masses of the Saturnian satellites, eccentricities, and inclinations are from Kozai (1957).

figures should not be considered fixed: for values of Q_p greater than the minimum values quoted in Eqs. (3) and (4), the origin should be moved appropriately to the right. The masses of the satellites used for these plots are shown in Table I. All of the first-order and some of the second- and third-order resonances that the Uranian and Saturnian satellites could have encountered due to tidal dissipation in the planet when the tidal dissipation function is independent of both amplitude and frequency are shown in Fig. 2.

General statements about capture into or passage through resonance while tidal torques are acting to change the ratio of the orbital periods can be made by considering the angular momentum exchanges needed to maintain exact resonance (Lissauer *et al.* 1984, Peale 1987). For satellites above synchronous height, the condition for the stability of a resonance demands that angular momentum be transferred from the inner to the outer satellite. Therefore, in discussing the dynamics of resonance, there are two types of orbital evolution that need to be considered. For satellites above synchronous height, permanent capture into resonance is possibly only if the orbit of the inner satellite is expanding faster than that of the outer satellite, that is, if the evolutionary paths of the satellites in Fig. 2 are converging with increasing time. If we write the ratio of mean motions as n'/n (<1), where the primed quantity refers to the mean motion of the outer satellite, then for satellites on converging orbits above synchronous height, n'/n increases with increasing time whereas the converse holds for satellites on diverging orbits. If the paths are diverging, then permanent capture into resonance is impossible and the satellite orbits must evolve, eventually, through any resonance that is encountered. Because of the strong decrease in the tidal torque with increasing distance from the planet, the evolutionary paths of satellites tend to converge as time increases. Exceptions to this rule occur when an outer satellite is so massive that the value of $m/a^{13/2}$ for this satellite exceeds that of its interior neighbor. This reversal probably occurs only for the satellite pairs Enceladus–Tethys and Miranda–Ariel.

Taking account of the strong a dependence of $(\dot{a}/a)_t$ as well as the possibility that

Q_p may not have been constant in the past, we estimate conservatively that for Mimas and Ariel

$$10^{-14} < (\dot{a}/a)_t < 10^{-12}, \tag{8}$$

where the unit of time is the orbital period of the satellite (~1–2 days).

III. DYNAMICS OF RESONANCE

Analytical Methods

To calculate the changes in the orbital elements that occur on encounter with a resonance, we must either use approximate analytical methods or resort to numerical integration. There are problems with both of these approaches. The approximate analysis of the dynamics of resonance has recently been very much simplified by the work of Henrard (1982) and Henrard and Lemaître (1983). This analysis relies on the averaging principle to truncate the perturbation Hamiltonian to a single term containing the resonant argument, as in Eq. (9) and Appendix A. Thus, close to the resonance the number of degrees of freedom is reduced to one. The phase space is therefore two dimensional and the Hamiltonian system can be described as moving on a closed trajectory in the phase plane. The effect of tides is to cause a slow variation of one of the parameters in this Hamiltonian. If the variation is sufficiently slow, then by the adiabatic theorem (see, e.g., Landau and Lifshitz 1960) the area enclosed by the trajectory is an invariant of the motion. As an illustration, consider the simple case of a $p{:}(p + q)$ e^q-type resonance described by an interaction Hamiltonian of the form

$$H' = -\frac{Gmm'}{a'} f(\alpha)e^q \times \cos(p\lambda - (p + q)\lambda' + q\tilde{\omega}), \tag{9}$$

where λ, λ' are the mean longitudes, $\tilde{\omega}$ is the argument of pericenter, $\alpha = a/a'$, and $f(\alpha)$ depends on Laplace coefficients. While the system is in a nonresonant state the area enclosed by the trajectory can be related directly to the mean value of the eccentricity of the inner satellite, so that $\langle e \rangle$ remains constant as the system evolves toward the resonance.

The adiabatic invariance of $\langle e \rangle$ breaks down when the resonance is encountered. In the case where tidal dissipation causes the orbits to diverge, $\langle e \rangle$ increases significantly on passage through the resonance in a time period of the order of the libration period T_l, and remains constant thereafter. The libration period T_l of the resonant argument is given by

$$T_l = T'\left[3(p + q)^2 \frac{m'}{M}(1 + g_r)\alpha f(\alpha)e^q\right]^{-1/2}, \tag{10}$$

where

$$g_r = \frac{m/m'}{\alpha}, \tag{11}$$

and T' is the orbital period of the outer satellite (see Appendix A). In the other case, where tidal dissipation causes the orbits to converge, there are two possible outcomes: resonant trapping or passage through resonance without capture. The probability of capture can be calculated analytically [see Malhotra (1988) and Appendix B]. If the system passes through resonance without capture, $\langle e \rangle$ undergoes a significant decrease over one libration period and remains constant thereafter, while if capture into resonance occurs, the forces exerted by the resonance act to increase $\langle e \rangle$ with time.

The physics of the phenomenon is expected to be described well in this manner provided that the interaction of the satellites is approximated well by the truncated Hamiltonian. The single most serious assumption that this entails is that the average motions of the nodes and pericenters are such as to make only one combination of angles have a near-vanishing frequency. This condition that the resonances are well separated in the frequency domain can be roughly quantified in terms of the libration widths. The libration width is the maximum variation in the ratio of the semimajor axes,

TABLE II

SATELLITE PARAMETERS

Satellite	$J_2(R_p/a)^2$ ($\times 10^5$)	$(B - A)/C$	e_{ov}
Miranda	0.136	0.025	0.19
Ariel	0.063	0.006	—
Umbriel	0.032	0.002	—
Titania	0.012	—	—
Oberon	0.007	—	—
Mimas	1.76	0.058	0.011
Enceladus	1.07	0.026	0.18
Tethys	0.70	0.016	0.47
Dione	0.43	0.005	—
Rhea	0.22	0.002	—

α, due to the resonant interaction of the satellites. It is given by

$$\Delta\alpha_l \approx 8\alpha\left[\frac{1}{3}\frac{m'}{M}(1 + g_r)\alpha f(\alpha)e^q\right]^{1/2}. \quad (12)$$

For example, the e^q and the I^q resonances are well separated if the separation of the exact resonance locations exceeds half the sum of the libration widths. This occurs if

$$z^q < \frac{3q^2J_2^2(R_p/a)^4}{4p^2(m'/M)(1 + g_r)\alpha[\sqrt{f_e(\alpha)} + \sqrt{f_I(\alpha)}]^2}, \quad (13)$$

where $f_e(\alpha)$ and $f_I(\alpha)$ refer to the e^q and I^q resonances, respectively, and for simplicity we assume that e and $\sin(\frac{1}{2}I)$ are of comparable magnitude and denote both by z. The inner Uranian satellites have both smaller values of $J_2(R_p/a)^2$ and larger mass ratios, m/M, than the inner satellites of Saturn (see Tables I and II). Thus, whereas the resonances in the Saturnian system are well separated, this is not always the case for resonances in the Uranian system (Dermott and Murray 1983, Dermott 1984a,b).

Resonances of particular interest in the Uranian system are the 3:5 resonance between Ariel and Umbriel and the 1:3 resonance between Miranda and Umbriel (see Fig. 2). These resonances were probably the most recent low-order resonances that the satellites encountered. In fact, if Q_p of Uranus is high, then they may have been the only low-order resonances that the satellites encountered. In this paper we focus on the 1:3 Miranda–Umbriel resonance, since this is the most likely candidate resonance for increasing both the eccentricity and the inclination of Miranda. The locations and widths of the various second-order resonances near the 3:5 commensurability between Ariel and Umbriel and the 1:3 commensurability between Miranda and Umbriel are shown in Fig. 3. The e'^2 and I'^2 resonances have been omitted, since we assume that these resonances have always been comparatively weak. For the ee' and the II' resonances, the vertical axis represents $\sqrt{ee'}$ and $\sqrt{II'}$, respectively. In using Fig. 3, it should be realized that resonance overlap can occur between resonances of quite disparate strengths (or libration widths), and that the dynamical significance

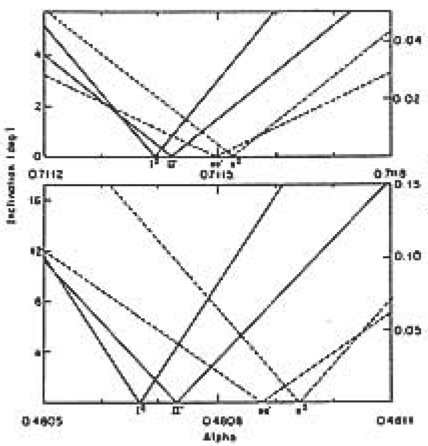

FIG. 3. Variations of libration widths with increasing eccentricities and inclinations for second-order resonances in the Uranian system. The upper panel describes the 3:5 resonances between Ariel and Umbriel; the lower panel refers to the 1:3 resonances between Miranda and Umbriel. For each satellite pair we show only the libration widths of the I^2, II', ee', and e^2 resonances. The I'^2 and e'^2 resonances located between the II' and ee' resonances are omitted. In the case of the mixed resonances, the vertical axis represents $(ee')^{1/2}$ and $(II')^{1/2}$, respectively.

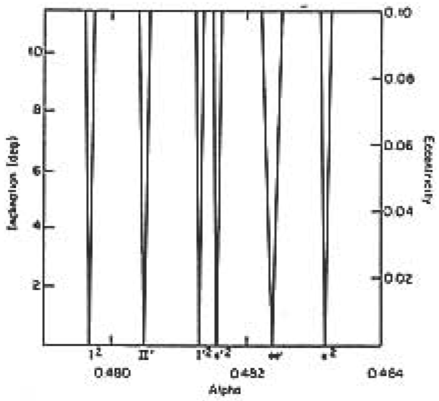

FIG. 4. Variations of libration widths for a second-order resonance in the Saturnian system. The resonance is the 1:3 resonance between Mimas and Dione. Compare this figure with that for the 1:3 resonance between Miranda and Umbriel shown in the lower panel of Fig. 3.

of resonance overlap depends on both the resonances involved and their relative strengths. The widths of the 1:3 Miranda–Umbriel resonances relative to their separations shown in the lower panel of Fig. 3 should be contrasted with those of corresponding resonances in the Saturnian system, the 1:3 Mimas–Dione resonances shown in Fig. 4. The effects of the bigger values of $J_2(R_p/a)^2$ and the smaller mass ratios, m/M, on the separation of the Uranian resonances are clear. Thus, while the single-resonance theory described above would be adequate for any of the Mimas–Dione 1:3 resonances, it may break down for the Miranda–Umbriel 1:3 resonances and for other low-order resonances in the Uranian system.

Numerical Methods

The numerical solution of the equations of motion presents difficulties of a different kind. If the satellite system has evolved over the age of the solar system, then the number of orbits that the satellites would have completed in that time is $\sim 10^{12}$. Accurate numerical integrations of this length are beyond the capability of any computer available today. We may hope to model the tidal evolution of the system by increasing $(\dot{a}/a)_t$ such that the interesting phenomena of resonance encounters in the past are hastened, and the number of orbits through which the system has to be evolved is manageable. However, if $(\dot{a}/a)_t$ is made too large, then the physics of the resonance encounter may be quite different.

We expect that the salient features of a resonance encounter can be reproduced with a higher value of $(\dot{a}/a)_t$ as long as this rate of evolution satisfies an adiabatic criterion in the vicinity of the resonance. A minimal requirement (adequate at least in the case of well-separated resonances) is that the change in the semimajor axis produced by tides in one libration period be much smaller than the amplitude of the oscillations in a due to the resonance:

$$\dot{a}_t T_l \ll \Delta a_l. \quad (14)$$

For an e^q resonance this condition is

$$\left(\frac{\dot{a}}{a}\right)_t \ll \frac{1}{T'} 8(p + q)\frac{m'}{M}(1 + g_r)\alpha f(\alpha)e^q. \quad (15)$$

This criterion is peculiar to each resonance and is more demanding for small e, particularly if the order of the resonance, q, is high.

To study the dynamics of a resonance encounter, numerical integrations need to be carried out over an interval many times the libration period. For $m'/M = 1.5 \times 10^{-5}$, $e = 0.01$, $p = 2$, and $q = 1$ numerical integrations have to be carried out for $\sim 10^5$ orbits. For a second-order resonance this estimate would have to be increased by a factor of 10. We have calculated the expected changes in the orbital elements on passage through first- and second-order resonances using the single-resonance theory and compared the results with those of accurate numerical simulations performed on the Cornell National Supercomputer. Figures 5 and 6 show the results of numerical integrations in which a pair of satellites is

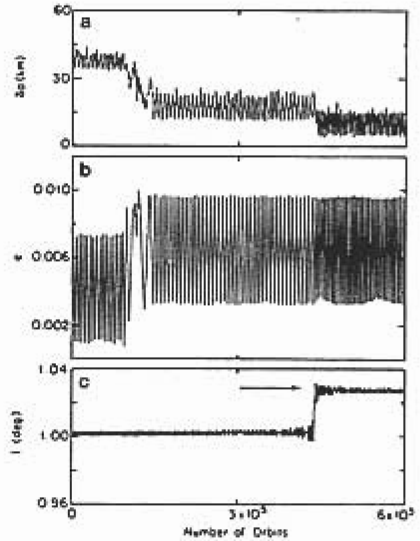

FIG. 5. Numerical results of passage through the 7:9 resonance with $(\dot{a}'/a')_t = 3 \times 10^{-9}$ under conditions for which the theory of Henrard and Lemaître (1983) is likely to apply. The unit of time is the orbital period of the outer satellite. To separate the e and I resonances, J_2 was set at the high value of 0.05. The other initial parameters were $m/M = 10^{-11}$, $m'/M = 10^{-4}$, $e = 0.0032$, $e' = 0.0023$, $I = 1.0°$, $I' = 0°$. The arrow in the bottom panel marks the inclination predicted by the theory after passage through the 7:9 I^2 resonance.

evolved through a second-order 7:9 resonance on diverging orbits. The value of $(\dot{a}'/a')_t$ was a factor of 5 lower than that necessary to satisfy the adiabatic criterion near the e^2 resonance. Figures 5a–c show the results of the integration when J_2 was given a value large enough to separate the e^2 and the I^2 resonances. The changes in e and I are in good agreement with those predicted by the theory. Figures 6a–c show the results for passage through the same resonance with the same value of $(\dot{a}'/a')_t$, when J_2 was reduced to 0.00335, the value appropriate for Uranus. Clearly, the theory breaks down in this case.

Figure 7 shows the increases in the eccentricity of Miranda due to passage through several successive resonances with Ariel. The increases in Fig. 7 were calculated numerically with $(\dot{a}'/a')_t = 1.6 \times 10^{-7}$, where the unit of time is the initial orbital period of Ariel. For $e = 0.02$, this value of $(\dot{a}'/a')_t$ is a factor of $\sim 10^2$ lower than that needed to satisfy the adiabatic criterion near the first-order resonances. The increases in e at the first-order and at some of the second-order resonances are in excellent agreement with the predictions of the theory shown in Fig. 7b. However, Fig. 7a does show one interesting and unexpected feature which, by repeated integrations, we have shown to be not at all atypical. Even though the satellites are on diverging orbits, on encounter with the 9:11 resonance between the 5:6 and 4:5 resonances, the satellites were trapped in an I^2 resonance. The satellites remained trapped in this resonance until the (simulated) tidal torque had acted to reduce I, after which escape occurred (see Fig. 7c). While the satellites remained trapped in the I^2 resonance, there were large-amplitude forced oscillations in the value of e.

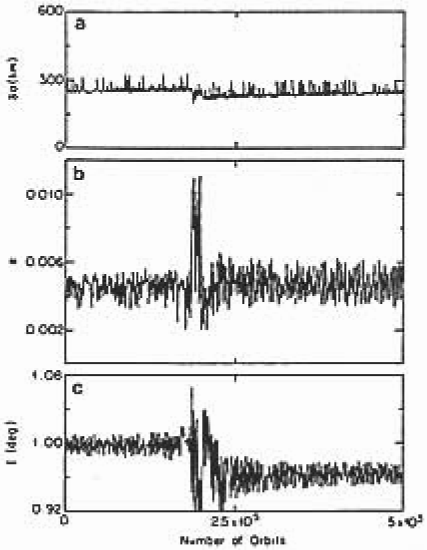

FIG. 6. Numerical results for passage through the 7:9 resonance with the same value of $(\dot{a}'/a')_t$ as that used in Fig. 5, but with $J_2 = 0.00335$ (a value appropriate for Uranus). The other initial parameters were $m/M = 8 \times 10^{-7}$, $m'/M = 1.5 \times 10^{-5}$ (these masses are appropriate for Miranda and Ariel), $e = 0.005$, $e' = 0.0001$, $I = 1.0°$, and $I' = 0°$. Contrast the decrease in Miranda's inclination with the predicted increase shown in Fig. 5.

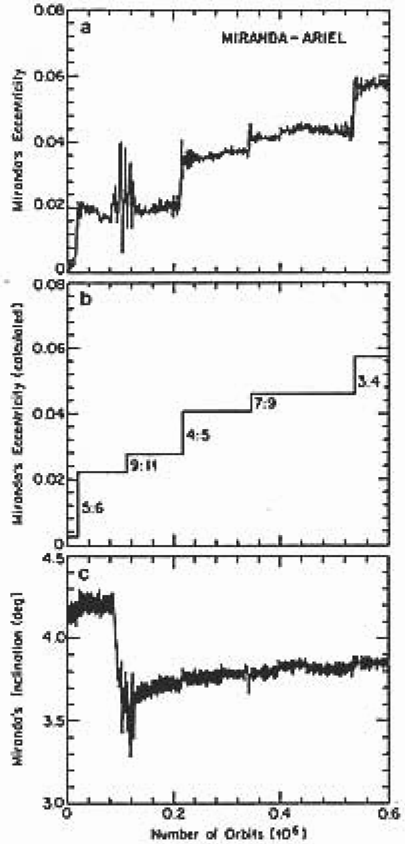

FIG. 7. (a) Increases in the orbital eccentricity of Miranda due to passage through resonances with Ariel found numerically with $(\dot{a}/a)_t = 1.6 \times 10^{-7}$ using the Cornell National Supercomputer (the unit of time is the initial orbital period of Ariel). This evolution rate is slow enough to determine those increases in e that occur at first-order resonances but not those that occur at all of the weaker resonances. This integration also includes increases in e due to tides raised on the planet, but does not include eccentricity damping due to tidal dissipation in the satellite. Since the satellites are on diverging orbits, permanent capture into resonance is impossible. However, we note large oscillations in e midway between the 5:6 and the 4:5 resonances. These are due to the temporary trapping of the satellites in a second-order (9:11) inclination-type resonance. (b) For comparison, we show the increases in e at first- and second-order resonances predicted by the theory of Henrard and Lemaître (1983). (c) The changes in Miranda's inclination. Note in particular, the large decrease in I that occurs on temporary trapping in the 9:11 I^2 resonance.

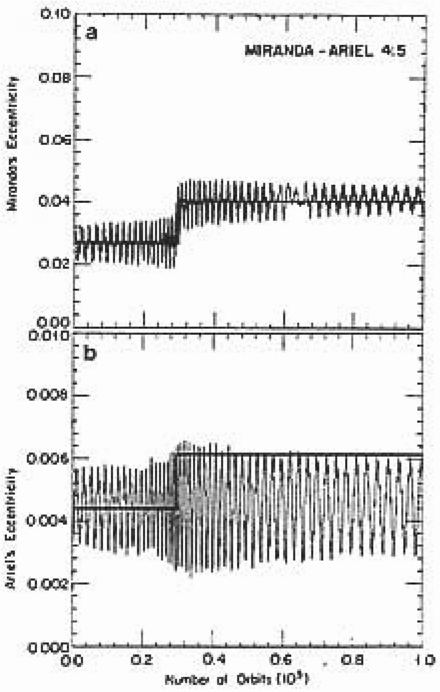

FIG. 8. Increase in the eccentricity of (a) Miranda and (b) Ariel due to passage through the 4:5 e and e' resonances found numerically with $(\dot{a}/a)_t = 5.5 \times 10^{-9}$ and $(\dot{a}'/a')_t = 4 \times 10^{-9}$ (the unit of time is 1.15 days) under conditions for which the e and e' resonances are not well separated. $J_2 = 0.00335$ (appropriate for Uranus), $m/M = 8 \times 10^{-7}$ (appropriate for Miranda), $m'/M = 1.5 \times 10^{-5}$ (appropriate for Ariel). The solid lines show the changes predicted by the theory of Henrard and Lemaître (1983).

A more detailed view of the increases in the eccentricities of both Miranda and Ariel on passage through the 4:5 resonance are shown in Fig. 8. In this integration the value of $(\dot{a}'/a')_t$ is a factor of $\sim 10^4$ lower than that necessary to satisfy the adiabatic criterion for the first-order e and e' resonances. The solid lines in Fig. 8 indicate the changes in e and e' predicted by the single-resonance theory. Evidently, even though the e and the e' resonances are not well separated, the theory works very well in predicting the increase in the eccentricity of Miranda on passage through the e resonance but fails completely to predict the change in Ariel's eccentricity on passage through the e' resonance. This could simply be a consequence of the fact that Miranda is less massive than Ariel and the theory is more appropriate in those circumstances. However, we note that since the satellites are on diverging orbits and α is increasing, the e resonance is encountered before the e' resonance. Since a significant decrease in α occurs on passage through the e resonance on a time scale of one libration period (see Fig. 5), one could argue that the contribution to $\dot{a}$ generated by passage through the e resonance is sufficient to ensure that the adiabatic criterion is violated on encounter with the e' resonance.

The results shown in Fig. 7 lead us to speculate that the peculiar thermal history of Miranda is a result of the fact that the satellite pair Miranda–Ariel evolves on diverging orbits. If the orbits of these satellites were much closer in the past, then tidal forces could have driven the satellites through a large number of first-, second-, and higher-order resonances in such a direction that permanent capture into resonance could not have occurred. As a result of this evolution, the eccentricity of the smaller, inner satellite could have increased to a comparatively large value if we neglect damping of the eccentricity due to tidal dissipation in the satellite (see Fig. 9). (We discuss this further in Section VII.) A similar argument can be made for Enceladus, since the satellite pair Enceladus–Tethys also evolves on diverging orbits. It is interesting that this argument can be applied only to Miranda and Enceladus. However, inspection of Fig. 2 shows that the satellite pairs Miranda–Ariel and Enceladus–Tethys could not have evolved through the resonances discussed above without other

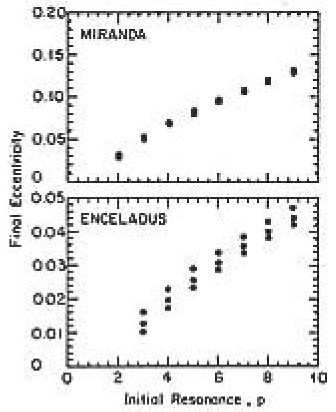

FIG. 9. Increases in eccentricity due to (1) passage through first- and second-order resonances calculated using the theory of Henrard and Lemaitre (1983) and (2) tides raised on the planet. The three sets of data points refer to initial eccentricities of 0, 0.005, and 0.01. In the case of Miranda, the final eccentricities are virtually indistinguishable. For a given initial eccentricity (0, 0.005, or 0.01) the value of the final eccentricity is determined by the starting point of the calculation. This is indicated here by the value of p for the first first-order resonance that the satellite passes through; that is, $p = 5$ indicates that the calculation is started just inside the 6:5 resonance. In the case of Miranda and Ariel, the calculation is continued until the satellites have passed through the 2:3 resonance. In the case of Enceladus and Tethys, the calculation is continued until the satellites have passed through the 3:4 resonance.

satellite pairs having passed through a number of first-order resonances for which capture may have been possible and, indeed, likely. We do not discuss these problems here, but note that an additional objection to the above evolutionary history of Miranda is that it does not account for the satellite's anomalously high inclination. Increases in the satellite's inclination could have occurred only on passage through the comparatively weak, second-order resonances and we find that the increase in Miranda's inclination that could have occurred due to the orbital evolution shown in Fig. 7 would not have amounted to more than a few tenths degrees. A more exact

value cannot be quoted since the second-order resonances are not well separated and the single-resonance theory cannot be applied. The more interesting case of the evolution of the orbital elements on capture into a resonance is discussed in the sections that follow.

IV. STRENGTHS OF RESONANCES

The stability of orbital resonances was first discussed by Goldreich (1965) who showed that the equation of motion for the resonant argument ϕ is approximated by the pendulum equation.

$$\ddot{\phi} = \pm\omega_l^2 \sin\phi + F, \tag{16}$$

where

$$F = p\dot{n}_t - (p + q)\dot{n}'_t, \tag{17}$$

and ω_l is the libration frequency [see Eq. (10) and Appendix A]. F is determined by the drag forces acting on the satellites. For the resonance to be stable against the disrupting effects of drag forces, the sign of $\ddot{\phi}$ must change. This requires that

$$|F| < \omega_l^2. \tag{18}$$

This criterion, which is approximately the same as the adiabatic criterion discussed in the previous section, is a condition on the eccentricities and inclinations. In general, we can write the resonant argument as

$$\phi = p\lambda - (p + q)\lambda' + q_1\tilde{\omega} + q_2\tilde{\omega}' + q_3\Omega + q_4\Omega'. \tag{19}$$

In those cases in which $|(\dot{n}/n)_t| \gg |(\dot{n}'/n')_t|$ and the equation of motion of ϕ is dominated by the mean motion terms, stability of the resonance demands that

$$\left(\frac{\dot{a}}{a}\right)_t < \frac{4\pi}{T'}(p + q)\frac{m'}{M} (1 + g_t)\alpha f(\alpha) e^{|k_1|} e'^{|k_2|} s^{|k_3|} s'^{|k_4|}, \tag{20}$$

where $s = \sin(\frac{1}{2}I)$.

In Table III, we show values of the eccentricities and inclinations, e_{stab} and I_{stab}, that are necessary for the stability of some of the many resonances that pairs of Uranian and Saturnian satellites could have encountered in the past while evolving on converging orbits. For odd-order resonances, we estimate I_{stab} from the strength of the eI^{q-1} resonance by assuming that $e \approx \sin(\frac{1}{2}I)$. It is clear from Table III that second- and even higher-order resonances cannot be dismissed from consideration on account of their lack of strength. This raises the question: Why are all but one of the observed resonances in the Jovian and Saturnian satellite systems of first order? One possible answer is that the probability of capture into resonance tends to decrease as the order of the resonance increases. In Section VIII we discuss another possibility, that is, the disruption of high-order resonances due to tidal dissipation in the satellite.

Capture into isolated first- and second-order resonances has been discussed by Henrard and Lemaitre (1983) [see also Borderies and Goldreich (1984)]. When tidal forces cause the orbits of two satellites to converge and to encounter a particular resonance, then capture into the resonance is a probabilistic event. The probability of capture depends on the value of the eccentricity (or inclination) before the resonance is encountered and is also a strong function of both the order of the resonance and the satellite masses. Capture into resonance is certain if the value of e (e', I, or I') is smaller than a critical value, e_{crit}. A summary of these results is given in Appendix B, and values of e_{crit} and I_{crit} for particular resonances are given in Table III.

The probabilities of capture into representative first- and second-order resonances are shown in Fig. 10 as functions of e, I, and m'/M (see also Appendix B). Values of m'/M in the Saturnian system range from 7×10^{-8} to 4×10^{-6}, whereas in the Uranian system we need only consider the case $m'/M = 1.5 \times 10^{-5}$ (see Table I). Note in particular the difference in the power dependencies of first- and second-order resonances with respect to the perturbing mass as well as e (or I). Although e_{crit}, for exam-

TABLE III

ECCENTRICITIES AND INCLINATIONS NEEDED FOR STABILITY AND CERTAIN CAPTURE[a]

Satellites	$p:(p+q)$	q	Resonance	e_{stab}	I_{stab} (deg)	z_{crit}	$(\dot{a}/a)_t$
Ariel–Umbriel	1:2	1	e	2×10^{-9}	—	0.028	9×10^{-7}
Miranda–Umbriel	1:3	2	e^2	8×10^{-5}	—	0.0065	3×10^{-10}
			I^2	—	0.01°	0.14°	1×10^{-7}
Ariel–Umbriel	3:5	2	e^2	2×10^{-5}	—	0.0043	8×10^{-9}
			I^2	—	0.003°	0.08°	3×10^{-10}
Ariel–Umbriel	4:7	3	e^2	5×10^{-4}	—	—	2×10^{-11}
			I^2	—	0.05°	—	2×10^{-12}
Mimas–Enceladus	1:2	1	e	2×10^{-7}	—	0.007	9×10^{-8}
	2:3	1	e	6×10^{-8}	—	0.005	3×10^{-7}
Tethys–Dione	2:3	1	e	5×10^{-9}	—	0.013	2×10^{-7}
Mimas–Enceladus	3:5	2	e^2	2×10^{-4}	—	0.0005	1×10^{-8}
			I^2	—	0.03°	0.01°	3×10^{-9}
Mimas–Tethys	1:2	1	e^2	1×10^{-4}	—	0.015	3×10^{-8}
	2:4	2	I^2	—	0.02°	0.048°	6×10^{-9}
Mimas–Dione	1:3	2	e^2	2×10^{-4}	—	0.0023	9×10^{-9}
			I^2	—	0.04°	0.05°	2×10^{-9}
Tethys–Dione	3:5	2	e^2	5×10^{-5}	—	0.002	5×10^{-13}
			I^2	—	0.01°	0.03°	2×10^{-11}
Dione–Rhea	3:5	2	e^2	3×10^{-5}	—	0.003	5×10^{-9}
			I^2	—	0.005°	0.05°	1×10^{-11}
Mimas–Enceladus	4:7	3	e^3	2×10^{-3}	—	—	7×10^{-10}
			eI^2	—	0.3°	—	3×10^{-10}
Mimas–Enceladus	5:8	3	e^3	2×10^{-3}	—	—	1×10^{-9}
			eI^2	—	0.2°	—	6×10^{-10}
Tethys–Dione	4:7	3	e^3	1×10^{-3}	—	—	1×10^{-12}
			eI^2	—	0.1°	—	1×10^{-10}
Tethys–Dione	5:8	3	e^3	1×10^{-3}	—	—	3×10^{-12}
			eI^2	—	0.1°	—	2×10^{-10}
Tethys–Dione	11:16	5	e^5	6×10^{-3}	—	—	2×10^{-16}
			eI^4	—	0.7°	—	7×10^{-13}

[a] Eccentricities and inclinations needed for stability, e_{stab} and I_{stab}, were calculated using $(\dot{a}/a)_t = 10^{-12}$ and $(\dot{a}'/a')_t = 0$ (see Eq. [20]). For odd-order resonances ($q = 3$ and 5), I_{stab} was estimated from the strength of the eI^{q-1} resonance by assuming that $e = \sin \frac{1}{2}I$. z_{crit} denotes the value of e or I below which capture into a resonance is certain. $(\dot{a}/a)_t$ is a measure of the tidal force that would disrupt a resonance assuming that the orbital elements are those listed in Table I.

ple, for a first-order resonance is much higher than that for a second-order resonance, the probability of capture falls off much faster for higher values of e in the case of first-order resonance. Thus, as Fig. 10 shows, when e is comparatively high the probabilities of capture into first- and second-order resonances are similar. Although we do not discuss the theory of capture into third- and higher-order resonances, these resonances should not, perhaps, be excluded from consideration. Since the number of resonant arguments associated with a commensurability increases markedly with the order of the resonance, then, for some range of e (and I), the probability that the system avoids capture into any resonance may even be smaller for a higher-order resonance.

The above discussion cannot be applied to resonances that are not well separated. This is the case for some second-order resonances in the Uranian system. If resonances are not well separated, then, as we

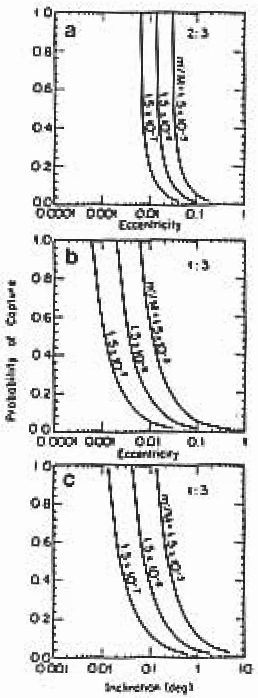

FIG. 10. The probability of capture into an isolated interior resonance. (a) A first-order e resonance for which $p/(p+q) = 2/3$. (b) A second-order e^2 resonance for which $p/(p+q) = 1/3$. (c) A second order I^2 resonance for which $p/(p+q) = 1/3$. The probabilities are calculated as functions of e or I for three values of the mass ratio m'/M with, in each case, the ratio of the satellite masses $m/m' = 0.1$.

have already seen (see Fig. 7), capture can occur in those circumstances in which the above theory would deem capture to be impossible. We emphasize these uncertainties in the capture process since temporary capture into a weak, high-order resonance could have a profound influence on the orbital and thermal evolution of a small, icy satellite.

V. EVOLUTION ON CAPTURE

Evolution on capture into resonance was first discussed by Allan (1969). He discussed the case of the well-separated, second-order, inclination-type resonances between Mimas and Tethys. However, his analysis is easily extended to any other type of isolated resonance in which the equation of motion of the resonant argument ϕ is dominated by the mean motion terms. For the purposes of this paper, these are the only cases of interest. Once capture into resonance occurs, the orbits of the satellites evolve while the ratio of their mean motions remains constant. This requires that the satellites exert a mutual torque that transfers angular momentum from the inner to the outer satellite at a rate determined by the tidal torques acting on the satellites. It is important to realize that the magnitude of the resonant torque between the satellites is independent of the strength of the resonance: if the order of the resonance is high, then the lag angle in the pendulum-like motion of the resonant argument is correspondingly large.

If, before the resonance is encountered, the orbits of the satellites are converging, then F in Eq. (16) is negative and evolution on capture always results in an increase in the orbital elements. For the resonant argument given by Eq. (19), the rates of change of the elements, to lowest order in e and I, are

$$\frac{\langle \dot{e} \rangle}{e} = -\frac{1}{e^2} q_1 \frac{m'}{M} na \frac{F}{3g} \tag{21}$$

$$\frac{\langle \dot{e}' \rangle}{e'} = -\frac{1}{e'^2} q_2 \frac{m}{M} n'a' \frac{F}{3g} \tag{22}$$

$$\frac{\langle \dot{I} \rangle}{I} = -\frac{1}{I^2} q_3 \frac{m'}{M} na \frac{F}{3g} \tag{23}$$

$$\frac{\langle \dot{I}' \rangle}{I'} = -\frac{1}{I'^2} q_4 \frac{m}{M} n'a' \frac{F}{3g} \tag{24}$$

where g is a positive constant given by

$$g = p^2 \frac{Gm'}{a^2} + (p+q)^2 \frac{Gm}{a'^2}. \tag{25}$$

We note that these rates are largely independent of the strength of the resonance, in the sense that the rates do not vary, for example, as e^q: the resonant argument

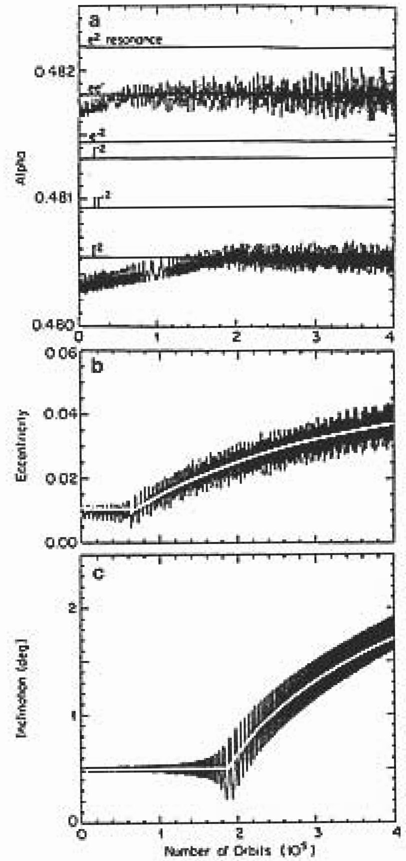

FIG. 11. Evolution of e and I on trapping in isolated, second-order resonances for which $p/(p+q) = 1/3$. The initial parameters used were $J_2 = 0.02$ (large enough to separate the eccentricity- and inclination-type resonances), $m/M = 8 \times 10^{-7}$, $m'/M = 3 \times 10^{-4}$ (a factor of 20 larger than the mass of Umbriel), $(\dot{a}/a)_t = 4 \times 10^{-9}$ and $(\dot{a}'/a)_t = 0$ (the unit of time is the initial orbital period of the outer satellite). The variations in alpha ($= a/a'$) shown in the top panel are for two separate numerical integrations. Note that these variations are less than the separations of the various second-order resonances. The middle panel shows the increase in e on trapping in the ee' resonance; the bottom panel shows the increase in I on trapping in the I^2 resonance. The white curves show the increases in e and I predicted by a low-order analytic theory (see Appendix A).

merely determines which elements are subject to change.

It is often the case that the torque on the inner satellite is much bigger than that on the outer satellite, in which case we can make the following approximations.

$$F = p\dot{n}_t = -3/2\, pna(\dot{a}/a)_t \tag{26}$$

$$g \simeq p^2(m'/M)n^2a. \tag{27}$$

Equation (21) then reduces to

$$\frac{\langle \dot{e} \rangle}{e} = \frac{1}{e^2}\frac{q_1}{2p}\left(\frac{\dot{a}}{a}\right)_t. \tag{28}$$

Similar approximations can be written for the other elements. It is evident that the eccentricity increases significantly on a time scale that can be very much shorter than the time scale over which tides act to expand the orbits of the satellites. This is discussed further in Section VII.

We also note that $\dot{e}$ is proportional to the order of the resonance, q. It would appear that high-order resonances are more effective at increasing the orbital elements than low-order resonances. Since $q/p = n/n' - 1$, it is correct to state that, so long as the stability condition described by Eq. (18) is satisfied, $\dot{e}$ is large when n/n' is large, that is, when the separation of the satellite orbits is large. This surprising result instructs us not to assume that interactions between near neighbors dominate the dynamical evolution of satellite systems: *some distant, outer satellite could have a marked influence on the dynamical evolution of an inner satellite.*

In Fig. 11 we show the results of a numerical simulation of the evolution that would occur on capture into a 1:3 resonance. In this integration we used a large value of J_2 to ensure that the sum of the resonance half-widths was less than the separation of the resonances. Also, by using a relatively large mass for the outer satellite (~20 times larger than that of Umbriel) we were able to use a correspondingly high value of $(\dot{a}/a)_t$ (3×10^{-9}) and thus produce large increases in e and I in a reason-

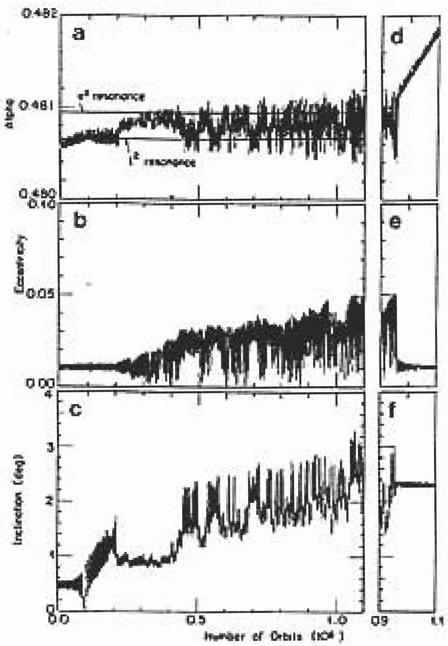

FIG. 12. Evolution of e and I on trapping in second-order resonances $p/(p+q) = 1/3$ that are not well separated. The parameters used were $J_2 = 0.003$ (appropriate for Uranus), $m/M = 8 \times 10^{-7}$, and $m'/M = 3 \times 10^{-4}$ (a factor of 20 larger than the mass of Umbriel). In (a)–(c), $(\dot{a}/a)_t = 2 \times 10^{-9}$ and $(\dot{a}'/a')_t = 0$. The unit of time is the initial orbital period of the outer satellite. (d)–(f) show a repeat of the evolution from orbit number 900,000 but with $(\dot{a}/a)_t$ increased to 10^{-8}. The integration was discontinued after the resonance disrupted.

able computation time. In Figs. 11b and c the system is trapped in the ee' and the I^2 resonances, respectively. (Note that Fig. 11 shows the results of two quite separate numerical integrations.) In this case we find that the increases in e and I are in very good agreement with the analysis given above.

In the above discussion, the various resonances are well separated. Next, we investigate the other situation in which the e^2 and I^2 resonances are of comparable strength but their separation is less than the sum of their half-widths. Figure 12 shows the results of a numerical integration simulating this case for a 1:3 resonance. The values of all quantities were the same as those in Fig. 11, except $J_2 = 0.003$ (similar to that of Uranus). In this case we find that the evolution is chaotic. Although the mean motions of the satellites remain near commensurate, the behavior is irregular and can best be described as a "hopping" from one type of resonance to another. As Fig. 13 indicates, the arguments corresponding to the different types of resonance exhibit intermittent circulating and librating motions. Figures 12b and c show the changes that occur in the eccentricity and inclination of the inner satellite while the near commensurability of mean motions is maintained.

On a closer examination of the evolution (see Fig. 14) one may make the following observations about this chaotic state of the system. The argument of the e^2 resonance, ϕ_6, librates whenever ϕ_1 (the argument of the I^2 resonance) circulates, and vice versa, although sometimes ϕ_5 (the argument of the

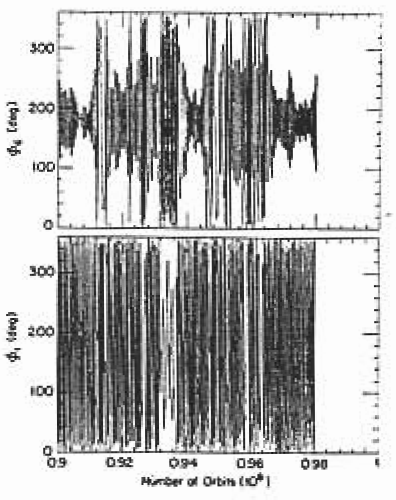

FIG. 13. Variations of the phases of the resonant arguments corresponding to the variations in e and I shown in Figs. 12b and 12c, respectively. ϕ_6 and ϕ_1 are the arguments of the e^2 and I^2 resonances, respectively. We note that when the argument of the e^2 resonance is librating, the argument of the I^2 resonance tends to be circulating, and vice versa.

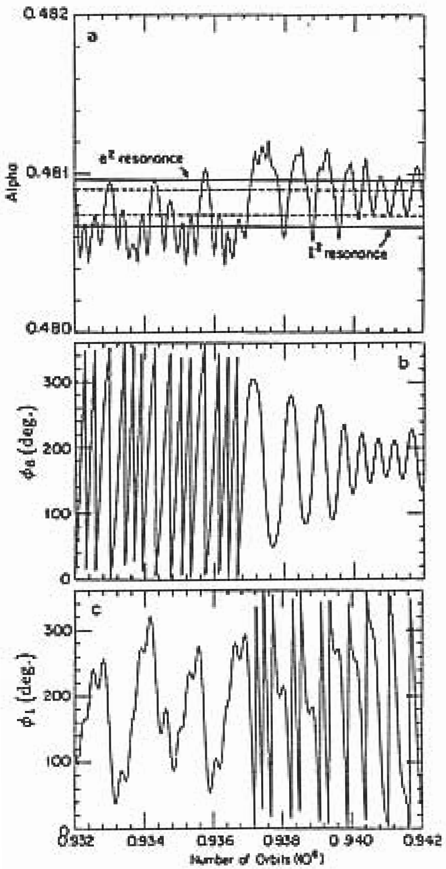

FIG. 14. An expanded view of the evolution of alpha between orbits 932,000 and 942,000 shown in Fig. 12a. The upper solid line in the top panel shows the location (or value of alpha) of the e^2 resonance, while the dashed line immediately below it shows the location of the ee' resonance. Similarly, the lower solid line shows the location of the I^2 resonance, while the dashed line immediately above it shows the location of the II' resonance. ϕ_6 and ϕ_1 are the arguments of the e^2 and I^2 resonances, respectively. We note that when the argument of the e^2 resonance is librating, the argument of the I^2 resonance is circulating, and vice versa.

ee' resonance) and ϕ_2 (the argument of the II' resonance) librate simultaneously with either ϕ_6 or ϕ_1, respectively. The mean value of the eccentricity e increases predominantly during those times when ϕ_6 librates, whereas the inclination increases predominantly during those times when ϕ_1 librates. However, we note that the eccentricity shows excursions to very small values for periods of time of the order of a libration period. We make the following empirical estimate for the changes in e and I that occur in this chaotic state:

$$\Delta e^2 \simeq r\Delta I^2, \tag{29}$$

where r is determined by the ratio of the total time spent in the e^2 resonance to the total time spent in the I^2 resonance. While the numerical experiments we have performed do not permit us to calculate the exact value of r, we estimate that its value is of the order of 1. We point out that this hopping behavior is quite surprising because, to second order in e and I, there is no coupling between the e^2 resonance and the I^2 resonance. Thus, an analytical or numerical investigation restricted to this order would not predict this phenomenon.

The single-resonance theory of Allan (1969) also describes the variation with time of the amplitude of libration of the resonant argument. The depth of the potential well that governs the pendulum-like motion of this argument is determined by the magnitude of e, e', I, or I'. Thus, the time scale of the rate of change of the amplitude of libration is always comparable to the time scale of the rate of change of the appropriate orbital element or elements which, in turn, is described by Eqs. (21)–(24). Figure 13 shows that when the resonances are not well separated and the motion is chaotic, this description of the evolution breaks down completely: large changes in the amplitude of libration occur on comparatively short time scales in a manner that cannot be described by the single-resonance theory. It is interesting, therefore, that while the pendulum-like description is clearly inadequate, the rates of change of e and I, after allowances have been made for the amounts of time spent in the appropriate resonant states, remain comparable to the rates predicted by the simple theory.

It is worth remarking on the locations of the exact resonances shown in Fig. 14. The predicted locations of the e^2 and I^2 resonances in this figure do not take into account the contributions to the pericenter and node rates arising from the resonant terms in the disturbing function. These contributions depend on the amplitude of libration of the resonant argument, and result in a decrease in the value of $\alpha_{\text{resonance}}$ which may be significant if the amplitude of libration is not too large. We have satisfied ourselves that these terms account for the discrepancies between the predicted and the observed resonant locations that are apparent in the figure. We digress to remark that in the case of a first-order resonance, the resonant contribution to the pericenter rate can be large and the effect that this term may have on the evolution of a resonance needs careful consideration, particularly in those cases in which tidal dissipation in the satellite acts to damp the eccentricity. Discussion of this is reserved for another paper.

In Figs. 12d–f we show the results of an integration in which the evolution shown in Figs. 12a–c was continued. This evolution was started at orbit number 900,000 with $(\dot{a}/a)_t = 10^{-8}$. In this run we observe the disruption of the resonance. Figure 15 shows a more detailed picture of this phenomenon. Just before disruption, while ϕ_6 was librating, e reached the relatively low value of 0.02. With this value of e, $(\dot{a}/a)_t$ is still a factor $\sim 10^2$ smaller than the critical value given by Eq. (20). We note that on disruption of the resonance, the inclination remained at the large value that it acquired during the chaotic state.

VI. THE MIRANDA–UMBRIEL 1:3 RESONANCE

The two cases studied in the previous section, in which the resonance widths are, respectively, smaller and greater than the separation of the resonances, are used here to describe the dynamics of the Miranda–Umbriel 1:3 resonance. If this resonance

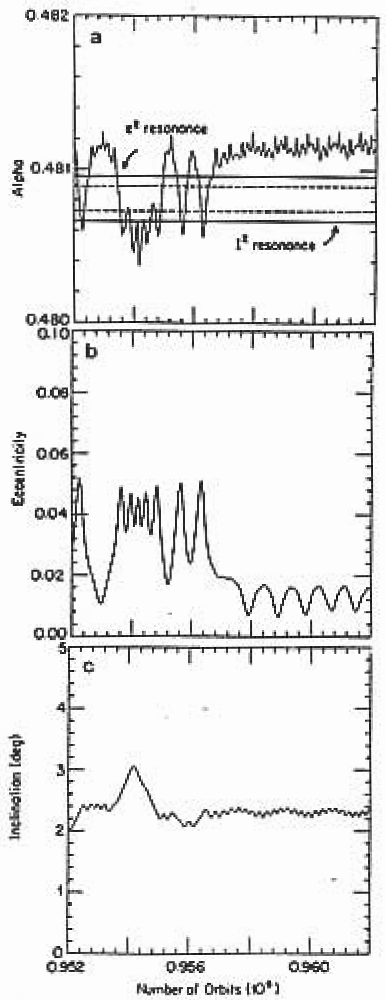

FIG. 15. An expanded view of the evolution of alpha, e amd I between orbits 942,000 and 952,000 shown in Figs. 12d–f in which we observe the spontaneous disruption of the resonance. The upper solid line in the top panel shows the location (or value of alpha) of the e^2 resonance, while the dashed line immediately below it shows the location of the ee' resonance. Similarly, the lower solid line shows the location of the I^2 resonance, while the dashed line immediately above it shows the location of the II' resonance. We note that disruption occurs when e is low (0.02), and that the value of I remains high after the disruption.

was responsible for increasing both the eccentricity and the inclination of Miranda, then it is probable, but not certain, that e and I were small before the resonance was encountered. As Fig. 3 indicates, for e and I small enough, the resonance widths are smaller than the separation of the resonances, so that the single-resonance theory is a good approximation. Tidal evolution toward this commensurability on converging orbits (α increasing) results in the I^2 resonance being encountered first. Capture into this resonance is certain if $I < 0.14°$, a value comparable to the present inclinations of the outer satellites. If capture occurs, then I increases at a rate given by Eq. (23). However, Tittemore and Wisdom (1987, Pasadena DPS Meeting) have found that, in the approximation of circular orbits, interference with the II' resonance may result in the I^2 resonance being disrupted when I reaches a value $\sim 4°$, similar to Miranda's present inclination. (This increase in I would occur in a time $\sim 6 \times 10^3 Q_p \gtrsim 10^8$ years). Indeed, Fig. 3 indicates that, if I' is small (but not zero), then resonance overlap between the I^2 and II' resonances could occur when I exceeds a value $\sim 4°$. Thus, we have a strong suggestion that Miranda's present inclination is the signature of this orbital resonance and that chaotic motion arising from resonance overlap led to the disruption of the inclination-type resonant state. According to the single-resonance theory, capture into the I'^2 resonance is certain only if $I' < 0.005°$. Thus, it is probable that capture into that resonance was avoided.

After escaping from the inclination-type resonances, the system evolves toward the eccentricity-type resonances. The e'^2 resonance is the first eccentricity-type resonance that would have been encountered, but capture into this resonance is certain only if $e' < 0.0002$. In contrast, for $e' = 0.004$ (the present value of Umbriel's eccentricity) capture into the ee' resonance is certain if $e < 0.008$ (Malhotra 1988), while capture into the e^2 resonance is certain if $e < 0.0065$. On capture into either of these resonances e must increase, although the rate of increase of e in the e^2 state is twice as great as that in the ee' state. As discussed in Section VII, if the satellite is cold, then in the isolated resonance approximation, the final eccentricity reached could be $\sim$0.1–0.2. However, from Fig. 3 we see that a modest increase in e results in the overlap of the e^2 and ee' resonances. For example, provided e' is not too small, interference between the e^2 and ee' resonances becomes significant for $e \gtrsim 0.03$. Figures 16 and 17 show examples of the types of behavior that could occur in the Miranda–Umbriel 1:3 resonance once resonance overlap occurs. In both of these integrations, Miranda's inclination was taken to be 4° and we have used the known masses of the satellites and a realistic value of $(\dot{a}/a)_t$, that is, 10^{-12}.

In Fig. 16 the initial value of e is comparatively small. Thus, the eccentricity resonances are isolated from the inclination resonances and we observe chaotic hopping only between the e^2 and ee' states. For the integration shown in Fig. 17, Miranda's initial eccentricity is high, 0.165. In this case, the e^2 and I^2 resonances overlap and we observe hopping between these, and the other, resonant states. The transition shown in Fig. 17 is particularly interesting: the system is seen to hop out of the I^2 resonance into a state in which the mean value of α is greater than that appropriate for any of the other possible resonant states. In this particular run, this transition did not lead to the disruption of the resonance; rather, the system hopped out of the nonresonant state back into the I^2 resonance. However, we consider it entirely probable that this type of transition could, eventually, result in the total disruption of the resonance.

In the following section we show that values of the eccentricity as high as 0.1–0.2 may not be unrealistic. However, the total length of the evolution of the 1:3 resonance between Miranda and Umbriel that we have investigated, some of which is shown in

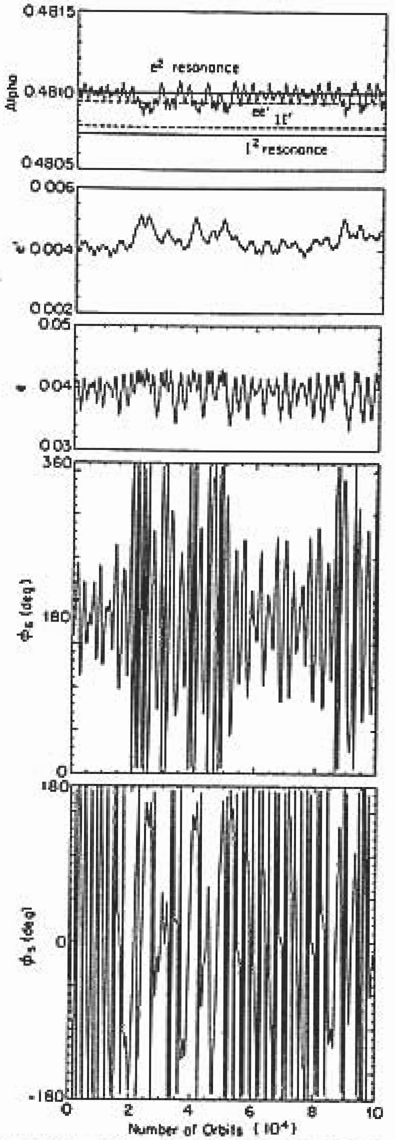

FIG. 16. Evolution of the Miranda–Umbriel 1:3 resonance when Miranda's eccentricity is high enough to cause overlap between the e^2 and the ee' resonances. All the other parameters of the integration are comparable to those of the real system: $m/M = 7.9 \times 10^{-7}$, $m'/M = 1.53 \times 10^{-5}$, $(\dot{a}/a)_t = 10^{-12}$, and $(\dot{a}'/a')_t = 0$. For this integration, the initial values of e, e', and I were 0.04, 0.004, and 4°, respectively.

Figs. 16 and 17, does not permit us to draw a clear conclusion about the likely final increase in Miranda's eccentricity. Although it is reasonable to assume that the eccentricity increases while the system remains in resonance and exhibits hopping between the various resonances, it is not possible for us to determine from these limited investigations the length of time that the resonance will avoid disruption. In particular, although we expect that resonance overlap does lead, eventually, to the total disruption of the resonance, at this stage of our work we do not know if this is likely to occur while there is overlap merely between the e^2 and ee' resonances, in which case the expected increase in e is modest, $\sim$0.03, or whether the resonance is likely to survive until the e^2 and I^2 resonances begin to overlap, in which case the expected increase in e would be large, $\gtrsim$0.1. It is evident that the dynamics is complex and requires a more detailed investigation than that attempted here. Numerical investigations for periods of 10^6 orbits can give only limited insight into the dynamical history of a system that is 10^{12} orbits old, particularly when that system is chaotic.

VII. TIME SCALES

To determine the effects that the resonance encounters described in the previous sections may have had on the orbital and thermal histories of the Uranian and Saturnian satellites, we need to evaluate the time scales of a number of significant processes. Heating a satellite by tidally damping its eccentricity may be an effective means of melting and resurfacing a satellite. However, before attempting to reach a conclusion on this matter we need to compare (a) the rate at which the eccentricity increases due to the action of the resonance with the rate of eccentricity damping due to tidal dissipation in the satellite and (b) the rate of heating in the satellite due to tidal dissipation with the rate at which heat is lost from its surface. For small, icy satellites, it is particularly important to realize that the

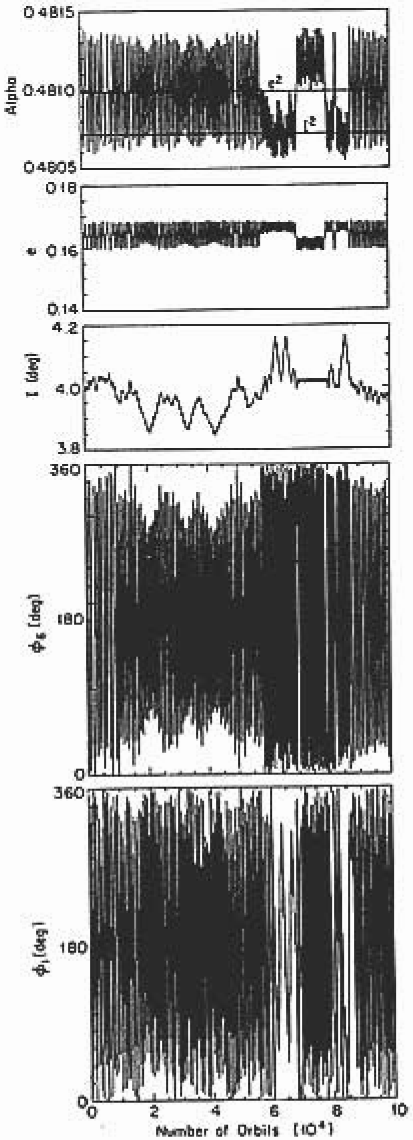

FIG. 17. Evolution of the Miranda–Umbriel 1:3 resonance when Miranda's eccentricity and inclination, e and I, are both high. All the other parameters of the integration are comparable to those of the real system: $m/M = 7.9 \times 10^{-7}$, $m'/M = 1.53 \times 10^{-5}$, $(\dot{a}/a)_t = 10^{-12}$, and $(\dot{a}'/a')_t = 0$. For this integration, the initial values of e and I were 0.165 and 4°, respectively. In this case, we observe chaotic hopping between a state in which the argument of the e^2 resonance, ϕ_6, is librating to a state in which the argument of the I^2 resonance, ϕ_1, is librating. We also observe hopping from a state in which the argument of the I^2 resonance, ϕ_1, is librating to a state in which alpha is above the libration zone and all the possible resonant arguments are circulating. In this case, however, the system then hops back into the I^2 resonance and disruption of the resonance does not occur.

tidal dissipation function may be temperature and thus time dependent.

Heating and Cooling

The heat generated in a satellite by the total damping of an eccentricity e is determined by the potential energy of the satellite in the gravitational field of the planet and is given by

$$\Delta E = e^2 \frac{GMm}{2a}. \tag{30}$$

We estimate that this heat is sufficient to raise the mean, internal temperature of Miranda by

$$\Delta T = 2 \times 10^4 e^2 \text{ K} \tag{31}$$

and that of Enceladus by

$$\Delta T = 6 \times 10^4 e^2 \text{ K}. \tag{32}$$

Here we have assumed that the mean specific heat of an icy satellite is $\sim 8.5T$ J kg^{-1} deg^{-1}, where T is the satellite's mean temperature (Hobbs 1974), and that $T \sim 150$ K. Since ΔE decreases inversely with distance from the planet, eccentricity damping is a particularly effective heating mechanism for satellites close to the planet.

The temperature increases needed to trigger endogenic processes such as satellite resurfacing depend on the satellite's composition, particularly its complement of volatiles. A eutectic melt of NH_3–H_2O forms at 175 K (Lewis 1971, Stevenson 1982). Thus $\Delta T \sim 100$ K could result in an interesting thermal event, whereas $\Delta T \gtrsim 200$ K may be necessary to produce significant melting in a satellite composed of pure water-ice. For Miranda, these temperature

increases require initial eccentricities of 0.07 and 0.1, respectively, whereas the same temperature increases would be achieved in Enceladus for initial eccentricities as low as 0.04 and 0.06, respectively. However, these temperature increases are achieved only if the eccentricity damping time scales of the satellites are considerably less than their characteristic cooling time scales.

The center of a homogeneous satellite cools by conduction on a time scale

$$\tau_c = \frac{R_s^2}{\pi^2 \kappa} \tag{33}$$

where κ is the thermal diffusivity (Carslaw and Jaeger 1947). Stevenson (1982) estimates that κ at 100 K for impure water-ice that contains dust particles, defects, and amorphous and vitreous phases is $\sim 2 \times 10^{-6}$ m^2 sec^{-1}, a factor of 2 lower than that of pure ice. Hence, for icy satellites with radii comparable to those of Miranda and Enceladus, $\tau_c \sim 10^8$ years. Once the central temperature exceeds about half the melting point of water-ice, then convection determines the heat transfer rate in the central regions of the satellite. However, we estimate that the overall cooling rate is not significantly affected unless the thickness of the nonconvecting mantle is less than about one-third the satellite radius.

For these comparatively small satellites, there are several reasons for arguing that the above cooling time scale is an underestimate. Recent papers by Klinger (1982), Smoluchowski (1983), Ahrens and O'Keefe (1985), and Lange and Ahrens (1987) have emphasized the effects of amorphous and porous ices on cooling time scales. The thermal conductivity of amorphous ice is lower than that of crystalline ice by at least a factor of 10. Amorphous ice forms on condensation from the vapor at temperatures below 150 K and could be a by-product of cratering events. It is likely that the debris produced by impacts is also highly porous. Dermott and Thomas (1988) have recently determined the moment of inertia of Mimas and shown that it is consistent with a deep, highly porous regolith. Porosity is retained in a cold, icy satellite until the overburden exceeds 50 bar and this occurs on satellites the size of Miranda only at depths greater than many tens of kilometers. A deep, porous regolith on a small, icy satellite could increase its cooling time scale by a factor of 10 or more. Thus, for Miranda and Enceladus we estimate, conservatively, that

$$10^8 \lesssim \tau_c \lesssim 10^9 \text{ years}. \tag{34}$$

Excitation and Damping of Eccentricities

Tidal dissipation in both the satellite and the planet results in a change in the eccentricity at a rate $\dot{e}_{\rm tidal}$ given by

$$\dot{e}_{\rm tidal} = \dot{e}_s + \dot{e}_p = -\frac{e}{\tau_{e,s}} + \frac{19}{8}\frac{e}{\tau_a} \tag{35}$$

where $\dot{e}_s$ is the rate of change of eccentricity due to tidal dissipation in the satellite alone and $\tau_{e,s}$ is the associated eccentricity damping time scale (Peale *et al.* 1980), $\dot{e}_p$ is the rate of change of eccentricity due to tidal dissipation in the planet, and τ_a is the time scale of orbital evolution due to tidal dissipation in the planet. Note that this equation is general in that we have not specified the spin state of the satellite; the subscript s is used merely to refer to the *satellite*.

On trapping in a resonance, the eccentricity changes at a rate $\dot{e}_r$ determined by F [see Eqs. (17) and (21)]. For simplicity, we neglect $(\dot{a}'/a')_t$ here and write

$$\dot{e}_r = \frac{1}{e}\frac{q}{2p}\left(\frac{\dot{a}}{a}\right)_{\rm total}. \tag{36}$$

The rate at which the eccentricity increases when a satellite is trapped in a resonance is determined largely by the rate at which tidal energy is dissipated in the planet. However, there is a contribution to $(\dot{a}/a)_{\rm total}$ due to tidal dissipation in the satellite. If the satellite is in either a synchronous or a chaotic spin state, and energy is dissipated in the satellite while the total angular momentum of the system is conserved, then it follows that

$$\left(\frac{\dot{a}}{a}\right)_s = 2e\dot{e}_s = -\frac{2e^2}{\tau_{e,s}}. \quad (37)$$

Thus the total $\dot{a}$ is given by

$$\left(\frac{\dot{a}}{a}\right)_{\text{total}} = \frac{1}{\tau_a}\left(1 - 2e^2\frac{\tau_a}{\tau_{e,s}}\right). \quad (38)$$

If tidal dissipation in the satellite is significant, then the eccentricity will be driven by the resonant torque to an equilibrium value e_{eq} for which $\dot{e}_{tidal} + \dot{e}_r = 0$. From Eqs. (35), (36), and (37), we obtain

$$e_{eq}^2 = \frac{q}{2(p+q)}\frac{\tau_{e,s}}{\tau_a}\left(1 - \frac{19p}{8(p+q)}\frac{\tau_{e,s}}{\tau_a}\right)^{-1}. \quad (39)$$

Note that e_{eq}^2 is proportional to q, the order of the resonance. Thus, a high-order resonance produces a higher final eccentricity than a low-order resonance.

For a satellite in synchronous rotation $\tau_{e,s} = \tau_{e,sync}$, where

$$\tau_{e,sync} = \frac{38a^2}{63n^3\rho_s R_s^4}\mu Q_s \quad (40)$$

where μ, ρ_s, R_s, and Q_s are the rigidity, density, radius, and tidal dissipation function of the satellite, respectively. This equation assumes that the deformation of the satellite is determined by elastic forces rather than by self-gravitation, i.e., that $\tilde{\mu} \gg 1$ where

$$\tilde{\mu} = \frac{57\mu}{8\pi G\rho_s^2 R_s^2}. \quad (41)$$

For an icy satellite of density 1.2 g cm^{-3} and radius 250 km, this requires that $\mu \gg 3 \times 10^7$ dyn cm^{-2}. In calculating the values of $\tau_{e,sync}$ listed in Table I, we have taken the rigidity of ice to be 4×10^{10} dyn cm^{-2}. However, the "effective" rigidity of a satellite may be considerably less than that of ice due to (1) the existence of a liquid core (Peale *et al.* 1979) and (2) the fact that the satellite may have been disrupted by cometary impacts and thus lack cohesive strength.

On trapping in an eccentricity resonance, the variation of the eccentricity with time is given by

$$e^2 = e_{eq}^2\left[1 - \exp\left(-\frac{t}{\tau_{eq}}\right)\right] \quad (42)$$

where, for a satellite in synchronous rotation, the time scale

$$\tau_{eq} = \frac{p}{2(p+q)} \times \left(1 - \frac{19p}{8(p+q)}\frac{\tau_{e,sync}}{\tau_a}\right)\tau_{e,sync}. \quad (43)$$

The eccentricity damping time scales, $\tau_{e,sync}$, for small, icy satellites the size of Mimas, Enceladus, Miranda, or Ariel are $\sim 3 \times 10^6 Q_s$ years (see Table I). The average value of τ_a is $\sim 3 \times 10^{10}$ years. However, resonances are most likely to be encountered when τ_a is a minimum. If we assume that $\tau_a \sim 10^{10}$ years and that $Q_s \sim 10^2$, then we estimate that for a 1:3 resonance, for example, $e_{eq} \sim 0.1$ and that the eccentricity would have increased to a value $0.8 \times e_{eq}$ in a time $\tau_{eq} \sim 5 \times 10^7$ years.

However, the above argument makes no allowance for the temperature dependence of Q_s. If the satellite is cold throughout when the resonance is encountered, and this is particularly likely for small satellites, then Q_s may be considerably greater than 10^2 and e_{eq} may be in the range 0.1 to 0.2. Eccentricity damping would become increasingly significant as the eccentricity increases and heat would be deposited in the satellite, preferentially in those locations where the strain rates are high—that is, at the center of the satellite. The melting of Io, as originally described by Peale *et al.* (1979), relied on a thermal runaway process. When the interior of the satellite started to melt, its "effective" rigidity was thereby reduced with the result that the dissipation rate in the remaining solid portion of the satellite was enhanced. This process could also occur in icy satellites. However,

it is enhanced by an even more effective process that does not depend on the interior being molten. Since the Q of ice decreases markedly with increasing temperature, most heat is produced in those portions of the ice that are warmest. This leads to a further decrease in the local value of Q and a thermal runaway. Once the above process is initiated in a satellite there is a marked decrease in its eccentricity damping time scale, with the result that the heat produced by the damping of its eccentricity is dumped in the satellite on a time scale less than or at least comparable to its cooling time scale, even after allowance has been made for the decrease in the latter due to the onset of convection in the interior.

VIII. CHAOTIC SPIN STATE

While a satellite is in either a nonsynchronous or a chaotic spin state, its tidal heating rate is increased by a factor of $1/e^2$. Noting this, Marcialis and Greenberg (1987) have proposed that episodes of chaotic spin may have been responsible for partially melting Miranda. In this section we show that it is possible that some of the small, inner satellites of Uranus and Saturn were knocked out of synchronous rotation by impacts not energetic enough to cause their disruption. However, it is not obvious that this will have any appreciable effect on the ultimate thermal state of the satellite. If the eccentricity damping time scale is less than the cooling time scale, then the temperature increase is only weakly dependent on these time scales. It must also be realized that we have no evidence or reason to believe that a satellite will remain in a chaotic spin state for a period much longer than its tidal despinning time scale (Wisdom 1987). Since the despinning time scale is less than the eccentricity damping time scale in the chaotic spin state by a factor $\sim 10^2$, it follows that the effect of an episode of chaotic spin on the thermal history of a satellite is probably minor. However, while the satellite is in a chaotic spin state, tidal dissipation in the satellite may appreciably enhance the orbital evolution rate and it is worth considering whether these enhanced orbital evolution rates could ever have been high enough to disrupt any of the possible orbit–orbit resonances.

We note that for a moderately deformed satellite, eccentricities of ~ 0.1 are comparable with the eccentricity e_{ov} necessary for the overlap of the synchronous spin state with the 3:2 spin–orbit resonance. Using the resonance-overlap criterion (Chirikov 1979, Wisdom *et al.* 1984), we estimate that

$$e_{ov} = \frac{1}{14}\left(\frac{n}{\nu_0} - 2\right)^2 \quad (44)$$

where the frequency of small-amplitude libration about the synchronous spin state, ν_0, is given by

$$\nu_0 = \left[3\frac{(B-A)}{C}\right]^{1/2} n. \quad (45)$$

A, B, and C are the principal moments of inertia of the satellite. Values of e_{ov} for some of the Uranian and Saturnian satellites are shown in Table II. The values of $(B - A)/C$ in this table are those expected for tidally and rotationally distorted satellites in synchronous rotation and near-hydrostatic equilibrium (Dermott and Thomas 1988).

The validity of the resonance overlap criterion can be determined by studying the appropriate surfaces of section. The surfaces of section shown in Fig. 18 depict the structure of the phase space for spin–orbit coupling for various values of $(B - A)/C$ and e. The spin axis of the satellite is assumed to be normal to its orbital plane—see Wisdom *et al.* (1984) for a detailed discussion of spin–orbit coupling. In Figs. 18a and b, $(B - A)/C = 0.06$, a value appropriate for Mimas, and perhaps Miranda too when it was closer to the planet. In Fig. 18a, $e = 0.02$, a factor of 2 greater than the value $e_{ov} = 0.009$ needed for resonance overlap, and we find that the island where libration about the synchronous spin state is possible is surrounded by an extensive

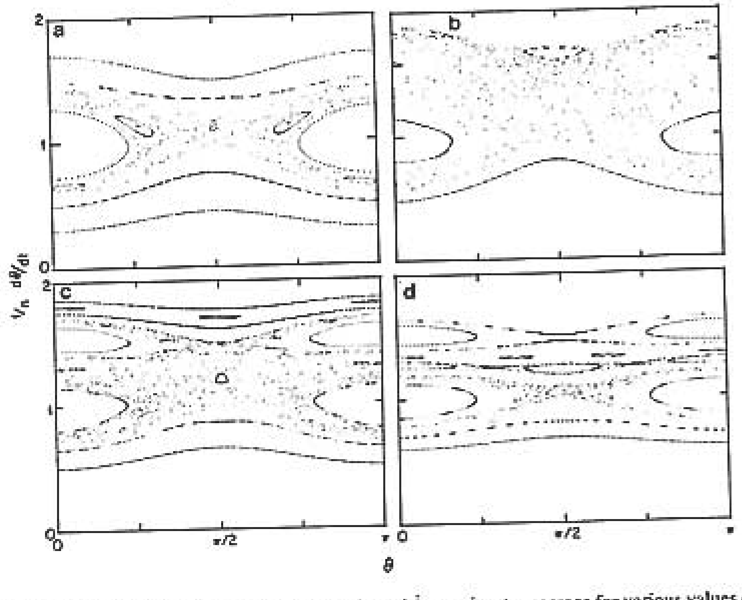

FIG. 18. Surfaces of section show the values of θ and $\dot\theta$ at pericenter passage for various values of $(B - A)/C$, and e. (a) $(B - A)/C = 0.06$, $e = 0.02$ (appropriate for Mimas). (b) $(B - A)/C = 0.06$, $e = 0.1$. (c) $(B - A)/C = 0.03$ (appropriate for Enceladus), $e = 0.1$. (d) $(B - A)/C = 0.015$ (appropriate for Tethys), $e = 0.1$.

region where the spin is chaotic. For higher values of the eccentricity, the region of regular librations shrinks while the chaotic region expands. In Fig. 18b, $e = 0.1$ and we find that the amplitude of libration cannot exceed 32° without the spin becoming chaotic. In Figs. 18c and d we show surfaces of section for very small values of $(B - A)/C$ and $e = 0.1$. The width of the chaotic region grows linearly with e, but it has an $\exp(-\pi n/2\nu_0)$ dependence as well and is thus highly sensitive to $(B - A)/C$. In Fig. 18c, $(B - A)/C = 0.03$, a value appropriate for Enceladus, while in Fig. 18d, $(B - A)/C = 0.015$, a value appropriate for Tethys. In both of these cases, e is substantially less than e_{ov} and yet we find that the island where libration about the synchronous spin state is possible is surrounded by an extensive chaotic sea. The amplitude of libration cannot exceed ~42° without the spin becoming chaotic.

That the motion of highly irregular satellites like Hyperion may be chaotic has been clearly demonstrated by the work of Wisdom *et al.* (1984). The implications of Fig. 18 are that when $(B - A)/C$ is very small, the resonance-overlap criterion underestimates the extent of the chaotic sea. Even if a satellite is near spherical, we must consider the possibility that if in the past its eccentricity was high, then its spin may have been chaotic. We do not imply by this that small-amplitude libration about the synchronous spin state is not possible for satellites in highly eccentric orbits. However, even a modestly deformed satellite could not be despun from a nonsynchronous state without passing through a substantial chaotic zone. This would occur not only on accretion (Wisdom 1987), but also on reaccretion if the satellite has been disrupted since the time of its formation. This may have been the case for some of the

small inner satellites of Uranus and Saturn (Smith *et al.* 1981, 1986). Another possibility, as we discuss below, is that impacting comets may have had sufficient angular momentum to knock the satellite into a chaotic spin state without the satellite being disrupted.

The effects of impacts on the spin rate of a satellite have received considerable attention recently. A review of this work has been given by Lissauer (1985) and by Chapman and McKinnon (1986). The increment $\Delta\nu$ in the spin rate of a satellite due to the impact of a comet of mass m and impact velocity v is given by

$$\Delta\nu = \frac{fmv}{\gamma m_s R_s} \sin\theta_1 \sin\theta_2, \qquad (46)$$

where θ_1 is the angle between the impacting comet's trajectory and the line from the satellite's center of mass to the point of impact, and θ_2 is the angle between the satellite's rotation axis and the plane defined by the impactor's trajectory and the line from the center of the satellite to the impact point (Lissauer 1985). $\theta_1 = 90°$ implies an impact at grazing incidence. $f(<1)$ is a factor that allows for the possibility that angular momentum may not be conserved in the impact, in the sense that material may be knocked off the satellite in the direction of motion of the impactor, particularly if θ_1 is close to 90° (Gault and Wedekind 1978).

Lissauer (1985) has shown that an impact will desynchronize a satellite if $\Delta\nu > \nu_0$, the librational frequency of the satellite's spin [see Eq. (45)]. If we assume that the satellite is in near-hydrostatic equilibrium, as Dermott and Thomas (1988) have shown to be the case for Mimas, then

$$\nu_0 = \left(\frac{45qH}{4}\right)^{1/2} n, \qquad (47)$$

where $q = 3n^2/4\pi G\rho_s$, and H (≤ 1) is a dimensionless constant determined by the satellite's internal density distribution (Dermott 1979b). For the purposes of this paper we assume $H = 0.85$, the value determined by Dermott and Thomas (1988) for Mimas.

A simple extension of Lissauer's argument shows that an impact will destabilize the spin of a satellite if

$$\Delta\nu > \nu_0 \sin\phi_c, \qquad (48)$$

where ϕ_c is the critical amplitude of libration derived from the width of the stable island associated with the synchronous spin state. This condition is satisfied if

$$mv > \frac{3}{2}\left(\frac{15H}{4\pi}\right)^{1/2} \frac{\gamma \sin\phi_c}{f \sin\theta_1 \sin\theta_2} \frac{m_s R_s n^2}{(G\rho_s)^{1/2}}. \qquad (49)$$

Since $\sin\phi_c < 1$, this condition is less demanding than that of Lissauer (1985) and becomes increasingly less demanding as e increases and the width of the stable island shrinks.

If we require that the satellite not be disrupted by the impact, then the impact velocity must be less than the limit v_l given by

$$\frac{1}{2} m v_l^2 < \frac{3}{5} \frac{G m_s^2}{R_s} \qquad (50)$$

where the right-hand side of the inequality is the satellite's gravitational binding energy. Since we have neglected the kinetic energy that is converted into heat, this must be regarded as an underestimate of v_l. For heuristic purposes, let us consider a "typical" impact for which $\theta_1 = 45°$, $\theta_2 = 60°$, $f = 1$, and $\phi_c = 32°$. Values of mv and v_l for some of the small, inner satellites of Uranus and Saturn are shown in Table IV. The im-

TABLE IV

IMPACTS NEEDED TO DISRUPT THE SYNCHRONOUS SPIN STATE[a]

Satellite	mv (cm g sec^{-1})	R_c (km)	v_l (km sec^{-1})	v_{orb} (km sec^{-1})
Mimas	7.6×10^{24}	12	8	14
Enceladus	9.3×10^{24}	13	22	13
Miranda	7.6×10^{24}	12	25	7

[a] mv is the momentum of an impactor needed to disrupt the synchronous spin state. The radius of the impactor, R_c, was calculated assuming a density of 1 g/cm³ and an impact velocity of 10 km/sec. An impact with velocity less than v_l and momentum mv will not disrupt the satellite. v_{orb} is the speed of the satellite in its orbit.

pactors needed to disrupt the synchronous spin states are certainly very large, but it is not clear to us that such impacts can be ruled out. For an impact speed of ~10 km/sec, for example, an impactor capable of disrupting the synchronous spin state must have a radius ≳12 km. In the cases of Enceladus and Miranda, such an impact would have insufficient energy to disrupt the satellite. However, even if the satellites were disrupted, then reaccretion would have occurred on a time scale less than that needed to circularize an eccentric ring of debris and the satellite would have been reformed in a nonsynchronous spin state with its orbital eccentricity intact.

A brief period of chaotic spin would have little effect on the thermal evolution of a satellite. However, while the satellite is not in the synchronous spin state, $(\dot a/a)_{\rm total}$ may be dominated by the term due to tidal dissipation in the satellite. From Eq. (38), we obtain

$$\left(\frac{\dot a}{a}\right)_{\rm total} = -\frac{2e^2}{\tau_{e,s}} = -\frac{2}{\tau_{e,\rm sync}}. \qquad (51)$$

If $Q_s \sim 10^2$, then $(\dot a/a)_{\rm total} \sim 4 \times 10^{-11}$ and could be as high as 10^{-10} if the interior of the satellite is warm. These drag rates are probably not high enough to disrupt any of the first- or second-order resonances, but they could be high enough to violate the stability condition [Eq. (20)] for some of the third- and higher-order resonances—see Table III.

From the equation of motion for the resonant argument, Eq. (16), we see that when $|F| > \omega_l^2$,

$$|\ddot\phi|_{\rm min} = |F| - \omega_l^2. \qquad (52)$$

Therefore, $|\dot\phi|$ must increase monotonically with time at least as fast as

$$|\dot\phi| = (|F| - \omega_l^2)t. \qquad (53)$$

For the resonance to be disrupted, $|F|$ must remain greater than ω_l^2 for a time t_c long enough to change $|\dot\phi|$ by an amount $\approx 2\omega_l$ so that in the subsequent evolution ϕ must circulate even if $|F| \to 0$. t_c is given by

$$t_c \approx \frac{2\omega_l}{|F| - \omega_l^2}. \qquad (54)$$

If the high value of $|F|$ is due to an episode of chaotic spin, then this high value will be sustained for a time of the order of the despinning time scale, $\sim 10^3$ years. For $|\dot a/a| \sim 10^{-10}$, t_c is of the order of tens of years for a third-order resonance. Thus, an episode of chaotic spin could ensure the disruption of high-order resonances. This could be an important reason for the complete absence of third- and higher-order resonances among the satellites.

IX. DISCUSSION

Motivation

The work described in this paper was motivated by the following considerations. In the Uranian satellite system, the high orbital inclination of Miranda is clearly anomalous. It is unlikely that an inclination as high as 4° and ~50 times bigger than the inclinations of the other satellites is primordial. Further, the eccentricities of the inner Uranian satellites, Miranda, Ariel, and Umbriel, are anomalously high considering their small eccentricity damping time scales. These time scales range from $1 \times 10^6 Q_s$ years for Ariel to $7 \times 10^6 Q_s$ years for Umbriel. If the tidal dissipation function of the satellite, Q_s, is $\sim 10^2$, then the observed eccentricities must be recent. It could be argued that this suggests a higher value of Q_s. However, since Q_s tends to unity as the melting point is approached, this argument is difficult to maintain for satellites such as Miranda and Ariel that have experienced major thermal events.

For these small, icy bodies, radioactive heating is an inadequate source of heat and we are aware of no other heating mechanism apart from eccentricity damping due to tidal dissipation in the satellite. Thus, the fact that the small, inner satellites have been resurfaced since the times of their last major bombardments also suggests that their eccentricities were considerably higher in the past.

Similar anomalies exist in the Saturnian satellite system. The eccentricity damping time scale of Mimas is $3 \times 10^6 Q_s$ years, yet its eccentricity is as high as 0.02. The small satellite Enceladus has clearly experienced a dramatic thermal event. The inclinations of Mimas and Tethys are 1.53° and 1.09°, respectively. These satellites are at present trapped in a second-order II' resonance, and Allan (1969) has demonstrated that the inclinations were probably smaller in the past. The initial inclinations of the satellites can be calculated from the present amplitude of libration of the resonant argument which is a well-determined quantity (97.040°). Since the initial amplitude of libration could not have exceeded 180°, it can be shown that the initial inclinations of Mimas and Tethys must have been greater than 0.4° and 1.0°, respectively (Allan 1969). We regard these initial inclinations, particularly that of Tethys, as anomalous, although, admittedly, they are not as extraordinary as the inclination of Miranda.

The spectacular tidal heating of Io was predicted on the basis of the resonant forcing of its eccentricity by Europa. As we have shown in Section V, an orbital resonance is an effective means of increasing the orbital elements. However, the features that we regard as anomalous in the Saturnian system cannot be accounted for by the present orbital resonances, while in the Uranian system there are no orbital resonances at all. It is our hypothesis that these features point to the existence of resonances in the past, in both of these systems, that have since been disrupted.

In the case of the Saturnian satellite system, further support for this suggestion can be obtained from consideration of (a) the formation of the observed resonances involving the satellite pairs Mimas–Tethys and Enceladus–Dione and (b) the satellite mass distribution. Goldreich (1965) suggested that the ratios of the orbital periods of these satellite pairs were originally random and that differential expansion of the satellite orbits was responsible for the formation of the present resonant configurations. However, inspection of Table I and Fig. 2 shows that the values of $m/a^{13/2}$ for these satellites are such that tidal evolution (with an amplitude-independent dissipation function Q_p) is quite ineffective in changing the *ratios* of their orbital periods. It is not possible to allow that the ratios of the periods of the satellite pairs Mimas–Tethys and Enceladus–Dione were more than a few percent different from their present values without also allowing that other satellite pairs evolved through a number of low-order resonances for which the probabilities of capture are high.

Evolution on Diverging Orbits

Differential tidal expansion of orbits causes satellites to encounter resonances on either converging or diverging paths. Since tidal torques decrease markedly with increasing distance from the planet, most pairs of satellites evolve on converging orbits. The two possible exceptions are the satellite pairs Miranda–Ariel and Enceladus–Tethys. These pairs of satellites could have evolved through resonances without permanent capture. Our numerical investigations show that when resonances are well separated, the increase in the eccentricity (or inclination) that occurs on passage through a resonance agrees well with the prediction of the approximate analytical theory. However, we find that when resonances are not well separated, as in the case of Miranda and Ariel, the increase in the eccentricity of the inner satellite is (in most cases) as predicted by the theory, but the theory breaks down completely in the case of the inclinations as well as in the case of the eccentricity of the outer, more massive satellite.

The increases in the eccentricities of Miranda and Enceladus that could have been produced by passage through a number of low-order resonances are high enough to be interesting. For a cold satellite, damping of the eccentricity between resonance encounters due to tidal dissipation in the satellite may not be significant until e is large. However, a problem with this scenario is that while these pairs of satellites could have passed through many resonances without capture to arrive at their present configurations, this evolution could not have occurred without other pairs of satellites encountering resonances for which capture would have been highly probable and may even have been certain. A further consideration is that this type of evolution, by itself, cannot account for the high inclination of Miranda.

Evolution on Converging Orbits

The existing resonances in the Saturnian system are all low order and well separated from nearby resonances with the same ratio of mean motions. Present theories of the tidal origin of these resonances appear to provide an adequate description of the evolution on capture. However, we have shown that many second- and higher-order resonances are also strong enough to withstand the forces exerted by tides. We need, therefore, to consider why all but one of the resonances in the satellite systems are first order (even the exception is only a second-order resonance). One possibility is that the probability of capture into a high-order resonance is small. On the other hand, there are many more resonances associated with a high-order commensurability than with a low-order one and the possibility that capture into a high-order resonance occurred in the past should be explored. In the work presented here we have focused on the 1:3 commensurability because this appears to be the most likely candidate for influencing Miranda's thermal and dynamical history. It is by no means the only high-order resonance of interest in the satellite systems of Saturn and Uranus. We have shown that once capture into a resonance occurs, then high-order resonances involving distant outer satellites are more effective than low-order resonances at increasing the eccentricities and inclinations.

Heating of Small Satellites

The evolution of the orbital eccentricity on capture into a resonance is determined by several competing processes. The time scales that determine this evolution are the eccentricity damping time scale due to tidal dissipation in the satellite, the cooling time scale, and the time scale on which the eccentricity increases due to the resonance. These time scales are comparable with each other, interrelated, and time (or temperature) dependent. They also determine the final, equilibrium value of the eccentricity, assuming that disruption of the resonance does not occur.

The eccentricity forced on the orbit of Io by Europa is low (0.0041). However, the eccentricity damping time scale of the satellite is also low (between $10^4 Q_s$ and $10^5 Q_s$ years) and the dramatic volcanism on Io has arisen because the resonance has, presumably, existed for a period much longer than many eccentricity damping time scales. The tidal heating of small, icy satellites demands a different scenario. We argue that on encounter with a resonance, satellites, particularly small satellites, may be cold throughout and that the value of Q_s may then be high ($>10^2$). Resonances are most likely to be encountered when the orbital expansion rate is at a maximum. These factors could operate together to ensure that the equilibrium eccentricity is high (>0.1). While the eccentricity damping rate is low, the resonance increases the eccentricity at a rate $\dot{e}/e$ that is a factor of e^{-2} greater than the orbital expansion rate, $(\dot{a}/a)_t$. Thus, large eccentricities could have been achieved on comparatively short time scales without significant eccentricity damping or heating of the satellite. The subsequent damping and warming of the satellite could lead to a marked reduction in both Q_s and the eccentricity damping time scale, with the result that significant heating could then occur on a time scale less than the cooling time scale.

If the satellite is in a nonsynchronous or

chaotic spin state, then the eccentricity damping time scale is drastically reduced. However, until we have evidence that a satellite is likely to remain in a chaotic spin state for periods substantially greater than the tidal despinning time, we cannot argue that episodes of chaotic spin are likely to have had a major influence on the thermal history of a satellite.

Chaotic Resonance

For eccentricities $e \gtrsim 0.03$, the dynamics of resonance in the Uranian and Saturnian satellite systems are quite different. The bigger values of the mass ratios m/M and the smaller value of J_2 in the Uranian system result in resonance overlap. Analytical theories that rely on a truncated Hamiltonian are no longer useful and we must resort to numerical methods. We have found that when resonance overlap occurs the system can exhibit several types of behavior.

In our first investigation we studied the case of a 1:3 resonance in which the e^2 and I^2 resonances were of comparable strength and the separations of the resonances were smaller than their widths. We found that capture took place in the I^2 resonance, and that the first transition into the e^2 resonance occurred when I had increased to a value sufficient for the overlap of the e^2 and I^2 resonances. Thereafter the system hopped between these resonant states, although libration of some of the other arguments sometimes occurred at the same time. While in this chaotic state, the eccentricity and inclination increased at comparable rates, not too different from those rates expected on the basis of the isolated resonance theory. We also observed the "spontaneous" disruption of this chaotic resonance. This occurred when $\dot{a}_t$ had a value approximately 100 times smaller than that required, on the basis of the simple strength criterion, Eq. (20), to disrupt the resonance.

The 1:3 resonance between Miranda and Umbriel, which may have been responsible for increasing both the eccentricity and the inclination of Miranda, was investigated under two different sets of circumstances. Using the simple analytical theory appropriate for isolated resonances, we described the order in which the resonances would have been encountered and those circumstances in which capture into the various resonances is likely to have occurred. If the initial inclination of Miranda was small ($<0.14°$), then capture into the I^2 resonance would have occurred first. On capture, the inclination I would have increased to $\sim 4°$ in $\sim 10^8$ years, after which overlap of the I^2 and the II' resonances would have occurred. Assuming, following Tittemore and Wisdom (1987), that chaotic hopping between these resonances results in the disruption of the inclination-type resonances, then further tidal evolution increases α until the eccentricity-type resonances are encountered.

If the eccentricities are small and the ee' and e^2 resonances are well separated, then the single resonance theory is valid. It predicts certain capture into the ee' resonance if $e < 0.008$ when $e' = 0.004$, and certain capture into the e^2 resonance if $e < 0.0065$. If Miranda is cold throughout, then it is reasonable to neglect tidal dissipation in the satellite in the first instance. In that case, Miranda's eccentricity increases to 0.03 in $\sim 10^5 Q_p$ years $\gtrsim 2 \times 10^7$ years. Overlap between the e^2 and ee' resonances is likely to occur when e reaches this value. We have shown that once overlap between e^2 and ee' resonances occurs, then the motion is chaotic and the system hops between these eccentricity-type resonances. If disruption does not occur, then we expect that Miranda's eccentricity increases to ~ 0.1 in $\sim 10^4 Q_p$ years $\gtrsim 2 \times 10^8$ years. Once the eccentricity of Miranda is as high as 0.1, while its inclination is $\sim 4°$, then the e^2 and I^2 resonances overlap and we have shown that hopping can then occur between the eccentricity- and inclination-type resonances. For one set of initial conditions we observed a curious hopping between the I^2

resonance and a state in which all the possible second-order resonant arguments are circulating. In this state the mean value of α is greater than the maximum value of α that is consistent with libration in the e^2 state. We think that it is this type of transition that results in the total disruption of the resonance. However, further investigations are required to determine if this is the case. Numerical integrations of the full equations of motion are valuable but their value is always limited by the fact that even with advanced computers it is difficult to explore the full range of solutions in a system that is dynamically very old.

The conditions under which the total disruption of the Miranda–Umbriel resonance is likely to occur are of particular interest since they probably determine the thermal history of Miranda. If it is necessary for the e^2 and I^2 resonances to overlap, then on disruption e would be large, $\gtrsim 0.1$, and eccentricity damping would result in a dramatic thermal event. Conversely, if overlap of the e^2 and ee' resonances is sufficient to ensure the total disruption of the resonance, then on disruption e is likely to be small, ~ 0.03. Damping of an eccentricity of this magnitude would result in a global temperature increase ~ 20 K. However, this argument assumes that tidal heating is uniform throughout the satellite. In fact, tidal strain rates are certainly not uniform. Furthermore, since the Q of ice is temperature dependent, a nonuniform tidal strain rate is sufficient to ensure that tidal heating is localized. The observed resurfacing on Miranda is confined largely to three coronae and is thus more suggestive of localized rather than global volcanism. If the heat derived from the damping of an eccentricity $e \sim 0.03$ is confined to 10% the volume of the satellite, then this is probably all that is required to account for the observations.

Disruption of a Resonance

The existence of various striking anomalies in the Uranian and Saturnian satellite systems has led us to suggest that resonances existed in the past in both of these systems that have since been disrupted. This hypothesis is untenable unless mechanisms exist for disrupting resonances. To put this problem in its proper context, we remark (a) that satellite systems are, dynamically, $\sim 10^2$ older than the planetary system and thus the long-term stability of satellite orbits may be less assured than those of the planets, and (b) that we are not concerned with the long-term stability of satellites in mundane orbits, but of those in resonant configurations. The long-term stability of these configurations, particularly those in which the resonances overlap and the motion is chaotic, is not known. This alone may account for the complete lack of orbit–orbit resonances in the Uranian system.

We have observed several spontaneous disruptions of chaotic resonances. One example is shown in Fig. 12. It would appear, however, that this and the other disruptions were partly a consequence of the high values of $(\dot{a}/a)_t$ that were used in some of our integrations. In Fig. 12 we observe that from time to time the eccentricity has excursions to very low values and that escape from the resonance occurred when e was at one of these lows. This and other numerical experiments suggest that the stability condition described by Eq. (20) overestimates, by a factor of $\sim 10^2$, the value of $(\dot{a}/a)_t$ that a resonance can withstand. However, again we must emphasize that this conclusion has been reached on the basis of investigations over $\sim 10^6$ orbits and that we do not know what value of $(\dot{a}/a)_t$ would effect the disruption of a chaotic resonance over a period as long as, say, 10^{10} orbits.

It is likely that the average value of $(\dot{a}/a)_t$ for tidally evolved inner satellites in both the Uranian and Saturnian systems is $\sim 10^{-12}$. Many high-order resonances, which tend to be well separated, particularly in the Saturnian satellite system, may be able to withstand these drag forces. However, we have pointed out that from time to time cometary impacts may dislodge small, nonspherical satellites from the synchronous spin state. We have shown that while the satellite is in a nonsynchronous spin state, $(\dot{a}/a)_t$ can be high enough to disrupt third- and higher-order resonances, even in the Saturnian satellite system.

Another mechanism for disrupting resonances that we have not discussed but that needs investigation involves the dynamics of satellites in one particular resonant configuration encountering other resonant configurations. Such a situation is likely to occur if a satellite system has undergone appreciable tidal evolution. This could be particularly important in the Saturnian satellite system. We must also remark that it is not known if the history of the 1:3 resonance between Miranda and Umbriel was divorced from that of the 3:5 resonance between Ariel and Umbriel. If these resonances were once exact, then the satellites would have been involved in a Laplace-type resonance for which

$$n_M - 3n_A + 2n_U = 0 \tag{55}$$

where n_M, n_A, and n_U are the mean motions of Miranda, Ariel, and Umbriel, respectively. Since the above relation is at present *almost* exact, we should consider the possibility that an exact Laplace-type resonance existed in the past.

To conclude, we consider that the present quiescent states of the satellite systems, particularly that of Uranus, are a poor guide to their orbital histories. It is plausible that some of the eccentricities were very much larger in the past and that the tidal damping of these enhanced eccentricities determined the dramatic thermal histories of some of the small, icy satellites.

APPENDIX A: ORBITAL EVOLUTION ON CAPTURE INTO RESONANCE

Consider two satellites of masses m and m' and position vectors $\mathbf{r}$ and $\mathbf{r}'$ with respect to a planet of mass M. Let a, e, I, $\tilde{\omega}$, Ω, and λ denote the semimajor axis, eccentricity, inclination, longitude of pericenter, longitude of ascending node, and mean longitude, respectively, of the mass m with similar primed quantities for the orbital elements of the mass m', where we assume $a' > a$. Lagrange's equations for the variation of the orbital elements of the mass m with time are given by (see, e.g., Brouwer and Clemence 1961)

$$\frac{dn}{dt} = -\frac{3}{a^2}\frac{\partial U}{\partial \lambda} \tag{A1}$$

$$\frac{de}{dt} = -\frac{\sqrt{1-e^2}}{na^2e}\left(1-\sqrt{1-e^2}\right)\frac{\partial U}{\partial \lambda} - \frac{\sqrt{1-e^2}}{na^2e}\frac{\partial U}{\partial \tilde{\omega}} \tag{A2}$$

$$\frac{dI}{dt} = -\frac{\tan\frac{1}{2}I}{na^2\sqrt{1-e^2}}\left(\frac{\partial U}{\partial \lambda} + \frac{\partial U}{\partial \tilde{\omega}}\right) - \frac{1}{na^2\sqrt{1-e^2}\sin I}\frac{\partial U}{\partial \Omega} \tag{A3}$$

$$\frac{d\varepsilon}{dt} = -\frac{2}{na}\frac{\partial U}{\partial a} + \frac{\sqrt{1-e^2}\left(1-\sqrt{1-e^2}\right)}{na^2e}\frac{\partial U}{\partial e} + \frac{\tan\frac{1}{2}I}{na^2\sqrt{1-e^2}}\frac{\partial U}{\partial I} \tag{A4}$$

$$\frac{d\tilde{\omega}}{dt} = \frac{\sqrt{1-e^2}}{na^2e}\frac{\partial U}{\partial e} + \frac{\tan\frac{1}{2}I}{na^2\sqrt{1-e^2}}\frac{\partial U}{\partial I} \tag{A5}$$

$$\frac{d\Omega}{dt} = \frac{1}{na^2\sqrt{1-e^2}\sin I}\frac{\partial U}{\partial I} \tag{A6}$$

where

$$\lambda = \int n dt + \varepsilon, \tag{A7}$$

n is the mean motion of the mass m, and U is the disturbing function given by

$$U = \mu' \left(\frac{1}{|\mathbf{r} - \mathbf{r}'|} - \frac{\mathbf{r} \cdot \mathbf{r}'}{r'^3} \right) \tag{A8}$$

with

$$\mu' = Gm'. \tag{A9}$$

There are similar equations for the variation of the orbital elements of the mass m' involving the disturbing function U' defined by

$$U' = \mu \left(\frac{1}{|\mathbf{r} - \mathbf{r}'|} - \frac{1}{r'} - \frac{\mathbf{r} \cdot \mathbf{r}'}{r^3} \right) \tag{A10}$$

with

$$\mu = Gm. \tag{A11}$$

U and U' can be expanded as a Fourier series in terms of the orbital elements of the masses m and m' (see, e.g., Kaula 1962, Allan 1969, Murray 1982).

With the exception of a few terms, which can be treated separately, the series expansions of U and U' have a similar form and a general resonant term can be written,

$$U = \mu' S \cos \phi \tag{A12}$$

$$U' = \mu S \cos \phi, \tag{A13}$$

where, to lowest order in the eccentricities and inclinations,

$$S = \frac{f(\alpha)}{a'} e^{|q_1|} e'^{|q_2|} s^{|q_3|} s'^{|q_4|}, \tag{A14}$$

and

$$\phi = p\lambda - (p + q)\lambda' + q_1\tilde{\omega} + q_2\tilde{\omega}' + q_3\Omega + q_4\Omega' \tag{A15}$$

with the D'Alembert relation requiring that

$$q = \sum_{i=1}^{4} q_i. \tag{A16}$$

Throughout this paper we will be considering only the lowest-order terms in the expansion of the disturbing function since we are interested only in applications to natural satellite orbits where the eccentricities and inclinations are small.

The function (α) depends on the ratio of the semimajor axes of the two bodies and on the particular resonance that is being considered. The sign of $f(\alpha)$, and hence the sign of S, determines the location of stable libration points. Although the sign can be determined by an analysis of the signs of the various functions, there is no simple rule for the general case (Ellis and Murray 1989).

For any given qth-order commensurability of the form p:$p + q$, a number of different resonances can exist, their exact locations being determined by their particular combinations of pericenters and nodes. As an example we will consider the 1:3 commensurability. There are six possible resonant angles in such a second-order resonance which we will number ϕ_1 to ϕ_6 in order of increasing values of α:

$\phi_1 = \lambda - 3\lambda' + 2\Omega$	I^2 resonance
$\phi_2 = \lambda - 3\lambda' + \Omega + \Omega'$	II' resonance
$\phi_3 = \lambda - 3\lambda' + 2\Omega'$	I'^2 resonance
$\phi_4 = \lambda - 3\lambda' + 2\tilde{\omega}'$	e'^2 resonance
$\phi_5 = \lambda - 3\lambda' + \tilde{\omega} + \tilde{\omega}'$	ee' resonance
$\phi_6 = \lambda - 3\lambda' + 2\tilde{\omega}$	e^2 resonance

(A17)

As the satellites evolve outward with increasing α they will encounter each of these resonances in turn.

If we denote the variation in the mean motions of m and m' due to tidal effects as $\dot{n}_t$ and $\dot{n}_t'$, respectively, then, from Eqs. (A1), (A12), and (A13) we have

$$\frac{dn}{dt} = \frac{3p\mu'}{a^2} S \sin \phi + \dot{n}_t \tag{A18}$$

$$\frac{dn'}{dt} = -\frac{3(p + q)\mu}{a'^2} S \sin \phi + \dot{n}_t'. \tag{A19}$$

Hence,

$$\ddot{\phi} = p\dot{n} - (p + q)\dot{n}' + q_1\ddot{\tilde{\omega}} + q_2\ddot{\tilde{\omega}}' + q_3\ddot{\Omega} + q_4\ddot{\Omega}' + p\ddot{\varepsilon} - (p + q)\ddot{\varepsilon}'. \tag{A20}$$

The terms on the right-hand side of Eqs. (A20) which involve second time derivatives are generally negligible and will be ignored for the moment. Thus,

$$\ddot{\phi} = 3gS \sin \phi + F, \tag{A21}$$

where

$$g = p^2 \frac{\mu'}{a^2} + (p + q)^2 \frac{\mu}{a'^2} \tag{A22}$$

and

$$F = p\dot{n}_t - (p + q)\dot{n}_t'. \tag{A23}$$

In resonance, the mean value of the second derivative of ϕ, $\langle\ddot{\phi}\rangle$ is zero, hence

$$\langle S \sin \phi \rangle = -(F/3g) \tag{A24}$$

and it is this equation that determines the lag angle. Using this result and Eqs. (A1)–(A8) we can derive expressions for the averaged values of the other orbital elements when a resonance condition holds. We find

$$\frac{\langle\dot{e}\rangle}{e} = -\frac{\mu'\sqrt{1 - e^2}}{na^2e^2} \left[q_1 + p(1 - \sqrt{1 - e^2}) \right] \frac{F}{3g} \tag{A25}$$

$$\frac{\langle\dot{e}'\rangle}{e'} = -\frac{\mu\sqrt{1 - e'^2}}{n'a'^2e'^2} \left[q_2 - (p + q)(1 - \sqrt{1 - e'^2}) \right] \frac{F}{3g} \tag{A26}$$

$$\frac{\langle\dot{I}\rangle}{\sin I} = -\frac{\mu'}{na^2\sqrt{1 - e^2} \sin^2 I} \left[q_3 + (p + q_1) \sin^2 \left(\frac{1}{2} I \right) \right] \frac{F}{3g} \tag{A27}$$

$$\frac{\langle\dot{I}'\rangle}{\sin I'} = -\frac{\mu}{n'a'^2\sqrt{1 - e'^2} \sin^2 I'} \left[q_4 + (q_2 - p - q) \sin^2 \left(\frac{1}{2} I' \right) \right] \frac{F}{3g}. \tag{A28}$$

To lowest order in the orbital elements, Eqs. (A25)–(A28) become

$$\frac{\langle\dot{e}\rangle}{e} = -\frac{1}{e^2} q_1 \frac{m'}{M} na \frac{F}{3g} \tag{A29}$$

$$\frac{\langle\dot{e}'\rangle}{e'} = -\frac{1}{e'^2} q_2 \frac{m}{M} n'a' \frac{F}{3g} \tag{A30}$$

$$\frac{\langle\dot{I}\rangle}{I} = -\frac{1}{I^2} q_3 \frac{m'}{M} na \frac{F}{3g} \tag{A31}$$

$$\frac{\langle\dot{I}'\rangle}{I'} = -\frac{1}{I'^2} q_4 \frac{m}{M} n'a' \frac{F}{3g}. \tag{A32}$$

We will now consider the question of the magnitude of the second-order derivatives that were neglected in deriving Eq. (A21). To simplify the analysis we will consider a general, internal, eccentricity resonance with resonant angle ϕ of the form

$$\phi = p\lambda - (p + q)\lambda' + q\tilde{\omega}. \tag{A33}$$

In this case it can be shown that the sign of S is determined purely by q, and S has the form

$$S = (-1)^q \frac{f(\alpha)}{a'} e^q, \tag{A34}$$

where $f(\alpha)$ is always taken to be positive and $q(>0)$ is the order of the resonance. (The analysis can easily be extended to include more general resonances.) Equation (A20) becomes

$$\ddot{\phi} = p\dot{n} - (p + q)\dot{n}' + q\ddot{\tilde{\omega}} + p\ddot{\varepsilon}. \tag{A35}$$

Using Eqs. (A1)–(A6) and (A34) with $q > 0$ we have, to lowest order in e,

$$\ddot{\varepsilon} = \frac{q}{4} \left(\frac{qS\mu'}{na^2e} \right)^2 \sin 2\phi \tag{A36}$$

and

$$\ddot{\tilde{\omega}} = \frac{(q - 2)}{2e^2} \left(\frac{qS\mu'}{na^2e} \right)^2 \sin 2\phi. \tag{A37}$$

Since $\ddot{\tilde{\omega}} \sim \ddot{\varepsilon}/e^2$, the $\ddot{\tilde{\omega}}$ term will always dominate over the $\ddot{\varepsilon}$ term in Eq. (A20) and the variation in ε can be ignored. Hence,

$$\ddot{\tilde{\omega}} \sim \mu'^2 e^{2q-4}, \tag{A38}$$

which implies that provided $q \gtrsim 2$ (i.e., a second- or higher-order resonance is being considered), the $\ddot{\tilde{\omega}}$ term is negligible. If $q = 1$ (i.e., a first-order resonance) then the motion of the pericenter can dominate the variation in ϕ for sufficiently low eccentricity. The critical value of e is given by

$$e_{\tilde{\omega}} = \left[\frac{\mu'^2 f(\alpha)}{6gn^2a^4a'}\right]^{1/3}. \tag{A39}$$

For $\mu' \gg \mu$ we have

$$g \sim \frac{m'}{M} p^2 n^2 a \tag{A40}$$

and

$$\alpha f(\alpha) \sim \tfrac{4}{5} p \tag{A41}$$

for large values of p. Hence,

$$e_{\tilde{\omega}} \sim \left[\frac{2}{15p}\frac{m'}{M}\right]^{1/3}. \tag{A42}$$

For $m'/M = 1.5 \times 10^{-5}$, $e_{\tilde{\omega}} < 0.01$ when $p \gtrsim 2$.

The square of the libration frequency [see Eq. (10) in the paper] is given by $3gS$. Thus, our expression for the libration period assumes that the equation for $\ddot{\phi}$ is dominated by the mean motion terms. The equation for $\ddot{\phi}$, Eq. (A21), can be integrated to obtain the energy integral and this can be used to place bounds on the variation of the semimajor axis [see Eq. (12) in the paper].

APPENDIX B: DYNAMICS OF RESONANCE PASSAGE

We present here a summary of the results of the application of the adiabatic invariant theory to the analysis of orbital resonances. For a review of the details see Peale (1986) and Malhotra (1988).

First-Order Resonance

We define the quantities

$$e_{\rm crit} = \left(\frac{2\sqrt{6}(m'/M)\alpha f(\alpha)}{p^2 + (p+1)^2(m/m')\alpha^2}\right)^{1/3} \tag{B1}$$

$$e'_{\rm crit} = \left(\frac{2\sqrt{6}(m/M)\alpha^3 f(\alpha)}{p^2 + (p+1)^2(m'/m)\alpha^4}\right)^{1/3}, \tag{B2}$$

where $\alpha = a/a'$; $f(\alpha)$ is a function of Laplace coefficients that has to be evaluated for each resonance; m, m', and M are the masses of the inner satellite, the outer satellite, and the planet, respectively; and p and $p + 1$ are integers describing the first-order resonance.

In the case where $(\dot{a}/a)_t < (\dot{a}'/a')_t$, the orbits of the satellites are diverging and capture into resonance is impossible. Passage through the e resonance results in an increase in e, while passage through the e' resonance results in an increase in e'. These increases are given here for the two limiting cases

$$x_i \ll x_{\rm crit}: \quad x_f = x_{\rm crit} \tag{B3}$$

$$x_i \gg x_{\rm crit}: \quad x_f^2 \simeq x_i^2 + \frac{8}{\sqrt{3}}\left(\frac{2}{3}\right)^{1/4}(x_i x_{\rm crit}^3)^{1/2} \tag{B4}$$

where x denotes e or e', and the subscripts i and f refer to values before and after passage through resonance.

In the other case when $(\dot{a}/a)_t > (\dot{a}'/a')_t$ and the orbits of the satellites are converging, capture into resonance is possible. The probability of capture, P_c, is given by

$$x_i < x_{\rm crit}: \quad P_c = 1 \tag{B5}$$

$$x_i \gg x_{\rm crit}: \quad P_c \approx \frac{2}{3^{3/4}\pi}\left(\frac{x_{\rm crit}}{x_i}\right)^{3/2}. \tag{B6}$$

Second-Order Resonance

In this case we define the following critical values:

$$e_{\rm crit} = \left(\frac{32/3(m'/M)\alpha f(\alpha)}{p^2 + (p+2)^2(m/m')\alpha^2}\right)^{1/2} \tag{B7}$$

$$I_{\rm crit} = \left(\frac{8/3(m'/M)\alpha f(\alpha)}{p^2 + (p+2)^2(m/m')\alpha^2}\right)^{1/2} \tag{B8}$$

$$e'_{\rm crit} = \left(\frac{32/3(m/M)\alpha^3 f(\alpha)}{p^2 + (p+2)^2(m'/m)\alpha^4}\right)^{1/2} \tag{B9}$$

$$I'_{\rm crit} = \left(\frac{8/3(m/M)\alpha^3 f(\alpha)}{p^2 + (p+2)^2(m'/m)\alpha^4}\right)^{1/2}. \tag{B10}$$

If the orbits are diverging then capture into resonance is impossible and the increase in the element x ($= e$, e', I or I') on passage through the appropriate resonance is given by

$$x_i \ll x_{\rm crit}: \quad x_f^2 \simeq x_{\rm crit}^2 - x_i^2 \tag{B11}$$

$$x_i \gg x_{\rm crit}: \quad x_f = x_i + \frac{2\sqrt{2}}{\pi}x_{\rm crit}. \tag{B12}$$

If the orbits are converging then capture into resonance is possible. The probability of capture is given by

$$x_i < x_{\rm crit}: \quad P_c = 1 \tag{B13}$$

$$x_i \gg x_{\rm crit}: \quad P_c = \frac{2\sqrt{2}}{\pi}\left(\frac{x_{\rm crit}}{x_i}\right). \tag{B14}$$

APPENDIX C: NUMERICAL METHODS

There are several methods available in the literature for the numerical integration of ordinary differential equations. Fox (1984) has compared several different single-step integrators for their performance in the integration of the equations of motion of celestial mechanics. He reported that among the more efficient routines were the Runge–Kutta–Dormand and the Gauss–Jackson methods. Since that comparative study was published, Everhart (1985) has presented another integrator based on the Gauss–Radau method. We have compared the Everhart and Runge–Kutta–Dormand routines (obtained from Fox) and found that Everhart's routine is somewhat superior in speed for the same level of accuracy.

The numerical integrations presented in this paper used Everhart's routine for the purpose of integrating a set of coupled differential equations of the specific form

$$\frac{d^2\mathbf{r}}{dt^2} = \mathbf{F}(\mathbf{r}), \tag{C1}$$

where $\mathbf{r}$ denotes a position vector. This routine uses Gauss–Radua spacings on each time step of the evolution. The integrator can be used in a constant-step-length or a variable-step-length mode. For the relatively small eccentricities and inclinations that we deal with in our application, and the relatively low accuracy that is required (since we are not doing ephemeris calculations we do not need global accuracy in the mean longitudes) the constant-step-length mode is very well suited. We used a step size of 1/20th of the orbital period of the innermost satellite. We performed checks on the accumulated global error in the time evolution of a single point-mass satellite in a Keplerian orbit about a point-mass planet. The error in the energy accumulates near-linearly with time.

For a system consisting of a "fixed" planet of mass M and two point-mass satellites, S_1 of mass m_1 and S_2 of mass m_2, the mutual gravitational forces lead to the following equations of motion for S_i:

$$\ddot{\mathbf{r}}_i^{(p)} = -\frac{G(M+m_i)}{r_i^3}\mathbf{r}_i - Gm_j\left(\frac{\mathbf{r}_i - \mathbf{r}_j}{|\mathbf{r}_i - \mathbf{r}_j|^3} + \frac{\mathbf{r}_j}{r_j^3}\right) \qquad i \neq j, \tag{C2}$$

where the origin of the coordinate system is fixed at the center of mass of the planet and the x–y plane is the equatorial plane of the planet.

The effect of the oblateness of the planet, J_2, is to produce a force per unit mass on the satellite S_i given by

$$\ddot{x}_i^{(\rm ob)} = -\frac{GM}{r_i^3}\left[\frac{3}{2}J_2\left(\frac{R_p}{r_i}\right)^2\left(1 - 5\frac{z_i^2}{r_i^2}\right)\right]x_i \tag{C3}$$

$$\ddot{y}_i^{(\rm ob)} = -\frac{GM}{r_i^3}\left[\frac{3}{2}J_2\left(\frac{R_p}{r_i}\right)^2\left(1 - 5\frac{z_i^2}{r_i^2}\right)\right]y_i \tag{C4}$$

$$\ddot{z}_i^{(\rm ob)} = -\frac{GM}{r_i^3}\left[\frac{3}{2}J_2\left(\frac{R_p}{r_i}\right)^2\left(3 - 5\frac{z_i^2}{r_i^2}\right)\right]z_i \tag{C5}$$

where R_p is the radius of the planet.

The effects of planetary tides were simulated by assuming that each satellite is affected only by the tide it alone raises on the planet. The tidal force per unit mass was taken to be

$$\ddot{x}_i^{(t)} = -\frac{m_i C_i}{r_i^8}y_i \tag{C6}$$

$$\ddot{y}_i^{(t)} = + \frac{m_t C_t}{r_i^3} x_i \tag{C7}$$

$$\ddot{z}_i^{(t)} = 0 \tag{C8}$$

where C_t is a constant depending on the planet's parameters. Thus, the equations of motion for the satellite S_i are

$$\ddot{\mathbf{r}}_i = \ddot{\mathbf{r}}_i^{(g)} + \ddot{\mathbf{r}}_i^{(ob)} + \ddot{\mathbf{r}}_i^{(t)}. \tag{C9}$$

All the integrations were performed on the Cornell National Supercomputer using the highest level of optimization. A typical run of 10^5 orbits took about 1 hr of CPU time, which is equivalent to about 100 hr of CPU time on a VAX/780 machine.

ACKNOWLEDGMENTS

We thank Keren Ellis for her help with Appendix A, Ken Fox for providing us with numerical integration codes, and Jeff Tennyson and Jack Wisdom for useful discussions. Much of this research was conducted using the Cornell National Supercomputer Facility, a resource of the Center for Theory and Simulation in Science and Engineering at Cornell, which is funded in part by the National Science Foundation, New York State, and the IBM Corporation. This work was also supported in part by NASA Grant NAGW-392 and by the UK Science and Engineering Research Council.

REFERENCES

AHRENS, T. J., AND J. D. O'KEEFE 1985. Shock vaporization and the accretion of the icy satellites of Jupiter and Saturn. In *Ices in the Solar System* (J. Klinger, D. Benest, A. Dollfus, and R. Smoluchowski, Eds.), pp. 631–654. Reidel, Dordrecht.

ALLAN, R. R. 1969. The evolution of the Mimas–Tethys commensurability. *Astron. J.* 74, 497–506.

ANDERSON, J. D., J. K. CAMPBELL, R. A. JACOBSON, D. N. SWEETNAM, A. H. TAYLOR, A. J. R. PRENTICE, AND G. L. TYLER 1987. Radio science with Voyager 2 at Uranus: Preliminary results on masses and densities of the planet and five principal satellites. *J. Geophys. Res.* 92, 14877–14883.

BORDERIES, N., AND P. GOLDREICH 1984. A simple derivation of capture probabilities for the $j+1{:}j$ and $j+2{:}j$ orbit–orbit resonance problems. *Celestial Mech.* 32, 127–136.

BROUWER, D., AND G. M. CLEMENCE 1961. *Methods of Celestial Mechanics.* Academic Press, New York.

CARSLAW, H. S., AND J. C. JAEGER 1947. *Conduction of Heat in Solids.* Oxford Univ. Press, London.

CHAPMAN, C. R., AND W. B. MCKINNON 1986. Cratering of planetary satellites. In *Satellites* (J. A. Burns and M. S. Matthews, Eds.), pp. 492–580. Univ. of Arizona Press, Tucson.

CHIRIKOV, B. V. 1979. A universal instability of many-dimensional oscillator systems. *Phys. Rep.* 52(5), 263–379.

DERMOTT, S. F. 1971. Atmospheric depths of Jupiter, Saturn, and Uranus. In *Planetary Atmospheres* (C. Sagan *et al.*, Eds.), pp. 371–374. Reidel, Dordrecht.

DERMOTT, S. F. 1979a. Tidal dissipation in the solid cores of the major planets. *Icarus* 37, 310–321.

DERMOTT, S. F. 1979b. Shapes and gravitational moments of satellites and asteroids. *Icarus* 37, 574–586.

DERMOTT, S. F. 1984a. Origin and evolution of the Uranian and Neptunian satellites: Some dynamical considerations. In *Uranus and Neptune* (J. Bergstralh, Ed.), NASA Conf. Pub. 2330, pp. 377–404.

DERMOTT, S. F. 1984b. The few body problem in celestial mechanics. *Nucl. Phys. A* 416, 535c–550c.

DERMOTT, S. F., T. GOLD, AND A. T. SINCLAIR 1979. The rings of Uranus: Nature and origin. *Astron. J.* 84, 1225–1234.

DERMOTT, S. F., AND C. D. MURRAY 1983. Nature of the Kirkwood gaps in the asteroid belt. *Nature* 301, 201–205.

DERMOTT, S. F., AND P. D. NICHOLSON 1986. Masses of the satellites of Uranus. *Nature* 319, 115–120.

DERMOTT, S. F., AND P. C. THOMAS 1988. The shape and internal structure of Mimas. *Icarus* 73, 25–65.

ELLIS, K., AND C. D. MURRAY 1989. Expansion of the disturbing function for external resonances. In preparation.

EVERHART, E. 1985. An efficient integrator that uses Gauss–Radau spacings. In *Dynamics of Comets: Their Origin and Evolution* (A. Carusi and G. B. Valsecchi, Eds.), pp. 185–202. Reidel, Dordrecht.

FOX, K. 1984. Numerical integrations of the equations of motion of celestial mechanics. *Celestial Mech.* 33, 127–147.

GAULT, D. E., AND J. A. WEDEKIND 1978. Experimental studies of oblique impact. *Proc. Lunar Planet. Sci. Conf.* 9, 3843–3875.

GOLDREICH, P. 1965. An explanation for the frequent occurrence of commensurable mean motions in the solar system. *Mon. Not. R. Astron. Soc.* 126, 257–268.

HENRARD, J. 1982. Capture into resonance: An extension of the use of adiabatic invariants. *Celestial Mech.* 27, 3–22.

HENRARD, J., AND A. LEMAÎTRE 1983. A second fundamental model for resonance. *Celestial Mech.* 30, 197–218.

HOBBS, P. V. 1974. *Ice Physics*, pp. 347–363. Oxford Univ. Press, London.

HUBBARD, W. B. 1984. Interior structure of Uranus. In *Uranus and Neptune* (J. Bergstralh, Ed.), NASA Conf. Pub. 2330, pp. 291–325.

KAULA, W. M. 1962. Development of the lunar and solar disturbing functions for a close satellite. *Astron. J.* 67, 300–303.

KLINGER, J. 1980. Influence of a phase change on the heat and mass balance of comets. *Science* 209, 271–272.

KLINGER, J. 1982. A possible resurfacing mechanism for icy satellites. *Nature* 299, 41.

KOZAI, Y. 1957. On the astronomical constants of the Saturnian satellite system. *Ann. Tokyo Astron. Obs. 2nd Ser.* 5, 73–106.

LANDAU, L. D., AND E. M. LIFSHITZ 1960. *Mechanics.* Pergamon, London.

LANGE, M. A., AND T. J. AHRENS 1987. Impact experiments in low temperature ice. *Icarus* 69, 506–518.

LASKAR, J., AND R. A. JACOBSON 1987. GUST86: An analytical ephermeris of the Uranian satellites. *Astron. Astrophys.* 188, 212–224.

LEWIS, J. S. 1971. Satellites of the outer planets: Their physical and chemical nature. *Icarus* 15, 174–185.

LISSAUER, J., S. J. PEALE, AND J. N. CUZZI 1984. Ring torque on Janus and the melting of Enceladus. *Icarus* 58, 159–168.

LISSAUER, J. J. 1985. Can cometary bombardment disrupt synchronous rotation of planetary satellites? *J. Geophys. Res.* 90, 11289–11293.

MALHOTRA, R. 1988. Some aspects of the dynamics of orbit–orbit resonances in the Uranian satellite system. Ph.D. thesis, Cornell Univ., Ithaca, NY.

MARCIALIS, R., AND R. GREENBERG. 1987. Warming of Miranda during chaotic rotation. *Nature* 328, 227–229.

MELOSH, H. J. 1975. Large impact craters and the moon's orientation. *Earth Planet Sci. Lett.* 26, 353–360.

MILANI, A., AND A. M. NOBILI 1985. The depletion of the outer asteroid belt. *Astron. Astrophys.* 144, 261–274.

MUNK, W. H., AND G. J. F. MACDONALD 1960. *The Rotation of the Earth.* Cambridge Univ. Press, Cambridge.

MURASE, T., AND A. R. MCBIRNEY 1973. Properties of some common igneous rocks and their melts at high temperatures. *Geol. Soc. Amer. Bull.* 84, 3563–3592.

MURRAY, C. D. 1982. Nodal regression of the Quadrantid meteor stream: An analytic approach. *Icarus* 49, 125–134.

MURRAY, C. D. 1986. The structure of the 2:1 and 3:2 Jovian resonances. *Icarus* 65, 70–82.

PEALE, S. J. 1977. Rotation histories of the natural satellites. In *Planetary Satellites* (J. A. Burns, Ed.), pp. 87–112. Univ. of Arizona Press, Tucson.

PEALE, S. J. 1986. Orbital resonances, unusual configurations and exotic rotation states among planetary satellites. In *Satellites* (J. A. Burns and M. S. Matthews, Eds.), pp. 159–223. Univ. of Arizona Press, Tucson.

PEALE, S. J. 1988. Speculative histories of the Uranian satellite system. *Icarus* 74, 153–171.

PEALE, S. J., P. M. CASSEN, AND R. T. REYNOLDS 1979. Melting of Io by tidal dissipation. *Science* 203, 892–894.

PEALE, S. J., P. CASSEN, AND R. T. REYNOLDS 1980. Tidal dissipation, orbital evolution, and the nature of Saturn's inner satellites. *Icarus* 43, 65–72.

SACKS, I. S., AND T. MURASE 1982. The anelasticity of peridotite and partial melt in the asthenosphere. Dept. Terrestrial Mag. Ann. Rep. 1982–1983. Reprinted from *Carnegie Inst. Washington Year Book* 82, 509–512.

SCHUBERT, G., T. SPOHN, AND R. T. REYNOLDS 1986. Thermal histories, compositions, and internal structures of the moons of the solar system. In *Satellites* (J. A. Burns and M. S. Matthews, Eds.), pp. 224–292. Univ. of Arizona Press, Tucson.

SINCLAIR, A. T. 1972. On the origin of the commensurabilities amongst the satellites of Saturn. *Mon. Not. R. Astron. Soc.* 160, 169–187.

SMITH, B. A., L. A. SODERBLOM, T. V. JOHNSON, A. P. INGERSOLL, S. A. COLLINS, E. M. SHOEMAKER, G. E. HUNT, H. MASURSKY, M. H. CARR, M. E. DAVIES, A. F. COOK II, J. BOYCE, G. E. DANIELSON, T. OWEN, C. SAGAN, R. F. BEEBE, J. VEVERKA, R. G. STROM, J. F. MCCAULEY, D. MORRISON, G. A. BRIGGS, AND V. E. SUOMI 1979. The Jupiter system through the eyes of Voyager 1. *Science* 204, 951–972.

SMITH, B. A., L. SODERBLOM, R. BEEBE, J. BOYCE, G. BRIGGS, A. BUNKER, S. A. COLLINS, C. J. HANSEN, T. V. JOHNSON, J. L. MITCHELL, R. J. TERRILE, M. CARR, A. F. COOK II, J. CUZZI, J. B. POLLACK, G. E. DANIELSON, A. INGERSOLL, M. E. DAVIES, G. E. HUNT, H. MASURSKY, E. SHOEMAKER, D. MORRISON, T. OWEN, C. SAGAN, J. VEVERKA, R. STROM, AND V. E. SUOMI 1981. Encounter with Saturn: Voyager 1 imaging science results. *Science* 212, 163–191.

SMITH, B. A., L. A. SODERBLOM, R. BEEBE, D. BLISS, J. M. BOYCE, A. BRAHIC, G. A. BRIGGS, R. H. BROWN, S. A. COLLINS, A. F. COOK II, S. K. CROFT, J. N. CUZZI, G. E. DANIELSON, M. E. DAVIES, T. E. DOWLING, D. GODFREY, C. J. HANSEN, C. HARRIS, G. E. HUNT, A. P. INGERSOLL, T. V. JOHNSON, R. J. KRAUSS, H. MASURSKY, D. MORRISON, T. OWEN, J. PLESCIA, J. B. POLLACK, C. P. PORCO, K. RAGES, C. SAGAN, E. M. SHOEMAKER, L. A. SROMOVSKY, C. STOKER, R. G. STROM, V. E. SUOMI, S. P. SYNNOTT, R. J. TERRILE, P. THOMAS, W. R. THOMPSON, AND J. VEVERKA 1986. Voyager 2 in the Uranian system: Imaging science results. *Science* 233, 43–64.

SMOLUCHOWSKI, R. 1983. Solar System ice: Amorphous or crystalline? *Science* 222, 161–163.

SQUYRES, S. W., R. T. REYNOLDS, P. M. CASSEN, AND S. J. PEALE 1983. The evolution of Enceladus. *Icarus* 53, 319–331.

Squyres, S. W., R. T. Reynolds, and J. J. Lissauer 1985. The enigma of the Uranian satellite's orbital eccentricities. *Icarus* **61**, 218–223.

Stevenson, D. J. 1982. Volcanism and igneous processes in small icy satellites. *Nature* **298**, 142–144.

Tennyson, J. L., J. R. Cary, and D. F. Escande 1986. Change of the adiabatic invariant due to separatrix crossing. *Phys. Rev. Lett.* **56**, 2117–2120.

Tittemore, W. C., and J. Wisdom 1987. Tidal evolution of the Uranian satellites. *Bull. Amer. Astron. Soc.* **19**, 821.

Wisdom, J. 1982. The origin of the Kirkwood gaps: A mapping for asteroidal motion near the 3/1 commensurability. *Astron. J.* **87**, 577–593.

Wisdom, J. 1983. Chaotic behavior and the origin of the 3/1 Kirkwood gap. *Icarus* **56**, 51–74.

Wisdom, J. 1987. Urey Prize Lecture: Chaotic dynamics in the Solar System. *Icarus* **72**, 241–275.

Wisdom, J., S. J. Peale, and F. Mignard 1984. The chaotic rotation of Hyperion. *Icarus* **58**, 137–152.

Yoder, C. F. 1973. *On the Establishment and Evolution of Orbit–Orbit Resonances.* Ph.D. thesis, University of California, Santa Barbara.

Yoder, C. F. 1979. How tidal heating in Io drives the Galilean orbital resonance locks. *Nature* **279**, 767–770.

Yoder, C. F., and S. J. Peale 1981. The tides of Io. *Icarus* **47**, 1–35.